Defence Research and Development Canada
Recherche et développement pour la défense Canada

DEFENCE R&D DÉFENSE

On the Implementation of Iterative Detection in Real-World MIMO Wireless Systems

Yvo de Jong

The work described in this document was partially sponsored by the Department of National Defence under Project No. 5CP.

Defence R&D Canada – Ottawa
TECHNICAL REPORT
DRDC Ottawa TR 2003-242

Communications Research Centre
CRC-RP-2003-009
December 2003

Canada

On the Implementation of Iterative Detection in Real-World MIMO Wireless Systems

Yvo de Jong
Communications Research Centre Canada

The work described in this document was partially sponsored by the Department of National Defence under Project No. 5CP.

Defence R&D Canada — Ottawa
TECHNICAL REPORT
DRDC Ottawa TR 2003-242

Communications Research Centre Canada
CRC-RP-2003-009
December 2003

Abstract

Theoretically, multiple-input multiple-output (MIMO) wireless systems can achieve remarkably high spectral efficiency as compared to conventional, single-antenna systems. This report identifies a number of problems which need to be solved in order to implement practical MIMO systems: channel estimation, correlated fading, slow fading, asynchronous reception, and frequency-selective fading. The effects of these non-ideal conditions on the performance of MIMO systems are evaluated, and directions are explored in which solutions may be found. The focus of the report is on MIMO systems employing an iterative ("turbo") receiver. The results presented are based on the iterative tree search (ITS) detection scheme developed recently at CRC, but are expected to be typical of most iterative detectors that have been proposed in the MIMO literature. The main conclusion of the report is that iterative channel estimation and further development of an ITS-based detection scheme for asynchronous and wideband reception are the two most promising topics for future research in this area.

Résumé

En principe, les systèmes sans fil multientrées et multisorties (MIMO) permettent une exploitation remarquable du spectre comparativement aux systèmes traditionnels à antenne unique. Le présent rapport recense un certain nombre de problèmes à résoudre avant de mettre en place des systèmes MIMO fonctionnels : estimation des voies, évanouissement corrélé, évanouissement lent, réception asynchrone et évanouissement progressif des fréquences. Il évalue les effets de ces conditions imparfaites sur le rendement des systèmes MIMO et examine des orientations qui pourraient donner des solutions. Le rapport se concentre sur les systèmes MIMO qui utilisent un récepteur itératif («turbo»). Les résultats présentés s'appuient sur la formule de détection de recherche arborescente itérative (RAI) élaborée dernièrement au Centre de recherches sur les communications, mais devraient ressembler à ceux de la majorité des détecteurs itératifs proposés dans la documentation sur les systèmes MIMO. Le rapport conclut notamment que l'estimation itérative des voies et le perfectionnement d'une formule de détection RAI pour la réception asynchrone et à large bande constituent les deux principaux sujets les plus prometteurs pour les futures recherches dans le domaine.

Executive summary

This report addresses the use of iterative detection in real-world multiple-input multiple-output (MIMO) wireless systems, which are theoretically capable of achieving remarkably high spectral efficiency through spatial multiplexing. A number of issues are identified which need to be overcome in order to implement practical MIMO systems, as discussed below. The focus of this report is on MIMO systems employing iterative ("turbo") receivers. The results presented herein are based on the iterative tree search (ITS) detection scheme developed recently at CRC, but are expected to be typical of most iterative MIMO detection schemes.

Channel estimation provides the detector with estimates of the MIMO channel matrix and the noise variance. If channel variations are sufficiently slow, channel training by means of the transmission of known pilot symbol vectors results in negligible performance loss compared to the hypothetical case of perfect channel knowledge, which is commonly assumed to be available. If the channel varies rapidly, the use of soft decision feedback is recommended in order to keep the training overhead acceptable. A method is discussed which is expected to overcome the vulnerability of existing soft decision feedback schemes to unreliable feedback. *Correlated fading* is well-known to degrade information-theoretic MIMO capacity, and, in addition, to decrease the efficiency of sub-optimal detection schemes such as ITS in approaching this theoretical limit. Although performance loss is inevitable in severely correlated fading, it is shown that the efficiency of ITS detection under such conditions can possibly be improved through asynchronous transmission, as discussed below. *Slow fading*, which is most likely to occur in indoor applications, enables accurate channel estimation with low training overhead, but is also shown to lead to performance degradation due to lack of temporal diversity. *Asynchronous reception*, which can occur, for example, in the downlink of networks with geographically distributed transmit arrays, precludes the use of existing MIMO detection schemes. It is possible to modify the ITS detector such that it can be applied in asynchronous scenarios. The modified scheme, called A-ITS, also enables intentionally asynchronous transmission, which, interestingly, results in considerable performance improvement. Because it is inherently capable of dealing with channels with memory, it is expected that A-ITS detection is also suitable for *frequency-selective fading* channels. Frequency diversity gains can possibly compensate for performance loss due to low temporal diversity, or can be traded off for lower receiver complexity.

The two most promising topics for future research concerning ITS-based MIMO detection are iterative channel estimation and the further development of the A-ITS scheme. The development of a suitable channel estimation scheme will remove the main obstacle in the implementation of practical MIMO systems based on the ITS detector. The use of A-ITS instead of synchronous ITS detection will increase the range of applications of ITS-based detection to include wideband and asynchronous scenarios, as well as schemes in which the number of transmit antennas exceeds the number of receive antennas, such as transmit diversity. Special attention will have to be paid to the relatively unexplored area of wideband and asynchronous channel estimation.

De Jong, Y.L.C. 2003. On the implementation of iterative detection in real-world MIMO wireless systems. DRDC Ottawa TR 2003-242. CRC-RP-2003-009. Communications Research Centre Canada.

Sommaire

Le présent rapport porte sur le recours à la détection itérative dans les systèmes sans fil multientrées et multisorties (MIMO) du monde réel qui permettent, en principe, une exploitation remarquable du spectre au moyen du multiplexage spatial. Il cible un certain nombre de problèmes à résoudre avant la mise en place de systèmes MIMO fonctionnels, dont il est question ci-dessous. Le rapport se concentre sur les systèmes MIMO qui utilisent un récepteur itératif («turbo»). Les résultats présentés dans ce rapport s'appuient sur la formule de détection de recherche arborescente itérative (RAI) élaborée dernièrement au Centre de recherches sur les communications, mais devraient ressembler à ceux de la majorité des formules de détection MIMO itérative.

L'*estimation des voies* fournit au détecteur des estimations de la matrice des voies MIMO et de la variation du bruit. Si les variations des voies sont suffisamment lentes, la formation des voies par la transmission des vecteurs symboliques pilotes connus cause une perte de rendement négligeable comparativement au cas hypothétique des connaissances des voies parfaites, dont la disponibilité est habituellement présumée. Si la voie varie rapidement, il est recommandé d'utiliser une contre-réaction à décision douce afin de conserver le niveau acceptable du surdébit de formation. Des discussions portent sur une méthode qui devrait permettre d'éliminer la vulnérabilité des formules existantes de contre-réaction à décision douce pour la contre-réaction peu fiable. Il est notoire que l'*évanouissement corrélé* dégrade la capacité MIMO théorique informationnelle et, en outre, diminue l'efficacité des formules de détection sous-optimales comme la recherche arborescente itérative (RAI) à l'approche de cette limite théorique. Bien que la perte de rendement soit inévitable lors d'un évanouissement fortement corrélé, des expériences ont démontré qu'il est possible d'améliorer l'efficacité de la détection RAI dans de telles conditions par la transmission asynchrone, tel qu'indiqué ci-dessous. L'*évanouissement lent*, qui survient très probablement dans les applications intérieures, permet une estimation précise des voies avec un faible surdébit de formation, mais cause aussi une dégradation du rendement en raison du manque de diversité temporelle. La *réception asynchrone*, qui survient notamment avec la liaison descendante des réseaux munis d'ensembles de transmission géographiquement dispersés, empêche l'utilisation des formules actuelles de détection MIMO. Il est possible de transformer le détecteur RAI de manière à l'appliquer à des scénarios asynchrones. La formule modifiée, appelée «A-ITS», autorise la transmission intentionnellement asynchrone, qui, de façon intéressante, améliore considérablement le rendement. Puisqu'elle est capable de traiter de façon inhérente avec des voies ayant de la mémoire, la détection A-ITS devrait aussi convenir aux voies d'*évanouissement progressif des fréquences*. Les gains de la diversité de fréquence peuvent compenser la perte de rendement causée par la faible diversité temporelle ou être échangés pour une complexité de récepteur plus basse.

Les deux principaux sujets les plus prometteurs pour les futures recherches sur la détection MIMO axée sur la RAI sont l'estimation itérative des voies et le perfectionnement de la formule A-ITS. L'élaboration d'une formule d'estimation des voies pertinente éliminera le principal obstacle de la mise en place de systèmes MIMO fonctionnels fondés sur le détecteur RAI. L'utilisation de la formule A-ITS au lieu de la détection RAI asynchrone fera croître la gamme d'applications de détection RAI afin d'inclure les scénarios asynchrones et à large bande et augmenter les formules pour lesquelles le nombre d'antennes de transmission excède le nombre d'antennes de réception, comme la diversité de transmission. Le domaine relativement inexploré de l'estimation des voies asynchrones et à large bande aura droit à une attention particulière.

De Jong, Y.L.C. 2003. On the implementation of iterative detection in real-world MIMO wireless systems. DRDC Ottawa TR 2003-242. CRC-RP-2003-009. Centre de recherches sur les communications Canada.

Table of contents

List of figures

List of Tables

Acknowledgement

The author thanks T.J. Willink (CRC) for her helpful comments.

1 Introduction

In recent years there has been much interest in wireless communication systems employing multiple antennas at both the transmitter and the receiver. This class of systems, commonly referred to as multiple-input multiple-output (MIMO), has the potential of achieving remarkably high spectral efficiency in rich multipath environments. The use of space-time bit-interleaved coded modulation (ST-BICM) in conjunction with an iterative receiver, in which soft-input soft-output detection and decoding stages exchange reliability information on the transmitted bits in an iterative fashion, has been shown to yield particularly good performance [1–7]. Under certain circumstances, e.g., turbo coding, rapid channel fading, and large interleaver depth, such systems can even approach the ergodic MIMO capacity limit [3].

As increased spectral efficiency is the primary reason for employing MIMO wireless systems, the use of a large number of antennas and high-order modulation such as 64-QAM is of special interest. Unfortunately, a problem with the optimum soft-input soft-output detector, the maximum *a posteriori* probability (MAP) detector, is that its computational complexity is exponential in the number of bits transmitted simultaneously in each symbol interval, which makes its application infeasible even for a moderate number of transmit antennas and/or modulation order. In order to solve this problem, several suboptimum, reduced-complexity detection schemes have been proposed; among them are the soft-cancellation minimum mean squared error (SC-MMSE) detector [4, 6, 7], the list sphere detector [3], and the iterative tree search (ITS) detector [1, 2, 8] developed at CRC. The complexity per bit of the ITS detector is only linear in N_t, and, if a special type of bit mapping called multilevel mapping is used, roughly independent of the modulation order. It has been demonstrated that, for the same computational complexity, the error performance of the ITS detector is comparable to or better than that of SC-MMSE and list sphere detection even for relatively small list sizes. This report focuses on the use of the ITS scheme.

In real-world MIMO systems, channel conditions are generally not as favourable as is often assumed for the sake of tractability and, also, knowledge of the channel state is not available *a priori*, but must be estimated using a suitable channel estimation scheme. Multipath propagation may lead to frequency-selective fading and, hence, inter-symbol interference, and the signals transmitted from different antennas may not be synchronized at the receiver. Furthermore, reduced diversity due to correlated and/or slow fading is known to degrade the performance of MIMO systems. The effects of such non-ideal conditions on the performance of MIMO systems employing ITS detection, and the question of how to deal with them in practical system implementations, have not been addressed to date. These issues are the topic of this report. The main aim herein is to identify problems that need to be overcome in order to implement a practical ST-BICM MIMO system based on ITS detection, and to explore directions in which solutions to these problems may be found.

The outline of the report is as follows. Section 2 reviews ST-BICM, iterative processing and MAP detection, and introduces notation that will be used in the rest of the report. The ITS detection scheme and its complexity and performance under ideal channel conditions are reviewed in Section 3. Section 4 contains the main contributions of this report. It identifies a number of issues that can impact practical MIMO systems based on ITS detection, provides an evaluation of their effects, and discusses approaches to deal with these issues. Final conclusions are drawn in Section 5.

2 Review of iterative MIMO detection and decoding

2.1 ST-BICM

Consider a MIMO system with N_t transmit antennas and N_r receive antennas ("$N_t \times N_r$ MIMO"), employing ST-BICM and an iterative receiver (see Fig. 2.1), and assume that $N_r \geq N_t$. Information bits are encoded, interleaved, serial-to-parallel converted and then mapped onto successive symbol vectors $\mathbf{s} = [s_1, \cdots, s_{N_t}]^T$ by the MIMO symbol vector mapper. The channel code can be an off-the-shelf code, e.g., a convolutional or turbo code. The modulation format is identical for all transmit antennas, and the number of bits per constellation point is denoted by M_c. In Fig. 2.1, the vector

$$\mathbf{x} = \left[x_{1,1}, \cdots, x_{1,M_c}, x_{2,1}, \cdots, x_{N_t,M_c}\right]^T \tag{2.1}$$

represents a block of $N_t M_c$ code bits from the output of the interleaver that is subsequently serial-to-parallel converted to N_t subblocks

$$\mathbf{x}_n = [x_{n,1}, \cdots, x_{n,M_c}]^T, \tag{2.2}$$

$n = 1, \cdots, N_t$, and then mapped onto $\mathbf{s}$ according to $s_n = \text{map}(\mathbf{x}_n)$. Here, $x_{n,k}$ denotes the kth bit mapped onto the nth symbol. For later convenience, the binary alphabet is defined by the set $\{-1, +1\}$.

In the following it is assumed that the channel, denoted by the $N_r \times N_t$ matrix $\mathbf{H}$, is random, frequency non-selective over the bandwidth of interest, and known perfectly at the receiver. The more realistic situation where only an imperfect estimate of $\mathbf{H}$ is available at the receiver is considered in Section 4.1. It is also assumed that $\mathbf{H}$ is full rank with probability one. The received signal vector is written as

$$\mathbf{y} = \mathbf{H}\mathbf{s} + \mathbf{n}, \tag{2.3}$$

where $\mathbf{n}$ is an additive noise vector whose elements are independent, complex-valued Gaussian variables with zero mean and variance σ_n^2. Eq. (2.3) represents a single use of the channel, which corresponds to the transmission of $N_t M_c$ code bits. The channel is accessed repeatedly to transmit a frame of bits typically spanning many vectors $\mathbf{x}$, and may vary from one channel use to the next. This is referred to as a block fading channel model in [5]. The depth of the interleaver is equal to the frame size, and is therefore typically much larger than $N_t M_c$.

2.2 Iterative processing

Iterative processing is a technique in which reliability information on the transmitted bits is exchanged between the detector and the channel decoder in an iterative manner, such that the decisions made by the channel decoder are improved by the detection process and vice versa. The detection and decoding stages in an iterative receiver must be capable of both accepting and producing soft information. and are therefore referred to as being soft-input soft-output. A block diagram of an iterative MIMO receiver is shown in the lower part of Fig. 2.1. The task of the MIMO detector is to provide updates, commonly called "extrinsic" information, L_E, on the soft-decision estimates of the code/channel bits. The computation of L_E is based on the received signal vector, $\mathbf{y}$, and any soft-decision bit information that may already exist. The latter information, called *a priori* information

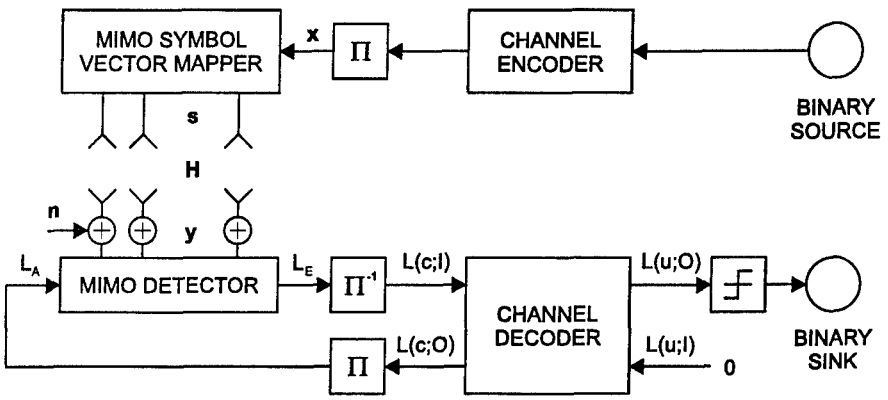

Figure 2.1. Block diagram of a MIMO system employing ST-BICM and an iterative receiver. Π and Π^{-1} denote interleaving and deinterleaving, respectively. $L(\cdot; I)$ and $L(\cdot; O)$ denote the soft inputs and outputs of the channel decoder, respectively. The letters c and u refer to coded and uncoded bits, respectively.

and denoted by L_A, becomes available at the output of the soft-input soft-output channel decoder after the first iteration, from where it is fed back to the detector input after being re-interleaved. The channel decoder is an algorithm that performs an update of the so-called *a posteriori* probabilities (APPs) of both the information and the coded bits based on the code constraint. In the case of convolutional coding, the decoding algorithm that is optimum in the sense that it maximizes the APP of each bit is the symbol-by-symbol MAP decoder, which is implemented efficiently in the BCJR algorithm [9]. In the case of turbo coding, which involves the parallel concatenation of two convolutional codes, the decoder is implemented by iterating the two symbol-by-symbol MAP decoders of the constituent codes [10]. Note that the receiver in an iterative MIMO system employing turbo coding performs two nested iterative procedures, the inner one associated with the turbo decoder and the outer one with the iterative detection and decoding process.

Generally, increasing the number of iterations in the detector/decoder loop improves the performance of an iterative receiver, but also increases its complexity proportionally. The optimum choice of the number of iterations is therefore determined by the receiver's convergence behaviour. This behaviour has been investigated experimentally for the soft-cancellation minimum mean squared error (SC-MMSE) detector [4, 6] and the MAP detector [5], discussed in Section 2.3. The results of these investigations are difficult to compare, because different numbers of transmit and receive antennas, channel coding schemes, interleavers, etc., were used. In all cases, however, complete convergence was reached after six or fewer iterations, while most of the gain with respect to non-iterative detection and decoding was obtained in the first two iterations, with diminishing gains in later iterations.

Theoretical studies concerning the convergence behaviour of iterative decoders and single-antenna iterative detection and decoding schemes have been reported in [11, 12], and were later extended for MIMO systems [13]. However, the method employed in these studies is based on an empirical characterization of the detector and decoder modules, by means of computer simulations. Although this method has been demonstrated to provide useful design guidelines for iterative systems, it does not provide any fundamental understanding as to how the design of the detector can improve the convergence properties of iterative MIMO receivers. The effect of the number of iterations on the error performance of an ST-BICM system employing the ITS detector will be investigated by computer simulations in Section 3.5.

2.3 MAP detection

The optimum detector in an iterative MIMO receiver is well known to be the MAP detector [3], sometimes also called APP detector. This detector computes extrinsic reliability information on the channel bits, expressed as log-likelihood ratios (LLRs), as

$$L_E(x_{n,k}) = \log \frac{\sum_{\mathbf{x} \in \mathbb{X}_{n,k}^{+1}} \exp\ \mu(\mathbf{s})}{\sum_{\mathbf{x} \in \mathbb{X}_{n,k}^{-1}} \exp\ \mu(\mathbf{s})} - L_A(x_{n,k}). \tag{2.4}$$

In this expression, $\log(\cdot)$ denotes the natural logarithm, and $\mathbb{X}_{n,k}^{+1}$ and $\mathbb{X}_{n,k}^{-1}$ are the sets of all possible bit sequences $\mathbf{x}$ for which $x_{n,k}$ is +1 and -1, respectively, i.e.,

$$\mathbb{X}_{n,k}^{\pm 1} = \left\{ \mathbf{x} \middle| \, x_{n,k} = \pm 1 \right\}. \tag{2.5}$$

The metric $\mu(\mathbf{s})$ in (2.4) is given by

$$\mu(\mathbf{s}) = -\frac{1}{\sigma_n^2} \left\| \mathbf{y} - \mathbf{H}\mathbf{s} \right\|^2 + \sum_{i=1}^{N_t} \sum_{j \in \mathbb{J}_i} L_A(x_{i,j}), \tag{2.6}$$

where

$$\mathbb{J}_i = \left\{ j \middle| \, j \in \{1, \cdots, M_c\} \text{ and } x_{i,j} = +1 \right\}. \tag{2.7}$$

The complexity of this detector is proportional to the number of different bit sequences contained in $\mathbb{X}_{n,k}^{+1}$ and $\mathbb{X}_{n,k}^{-1}$, which is equal to $2^{N_t M_c}$. This property makes the use of MAP detection impractical, especially if the number of transmit antennas and/or the signal constellation size are large.

3 Iterative tree search detection

The suboptimum ITS detection scheme proposed herein has a much lower complexity than the MAP detector of Section 2.3 as it evaluates only the bit sequences $\mathbf{x}$ that contribute significantly to the detector output (2.4), i.e., those for which the metric $\mu(\mathbf{s})$ is "large". To this end, in each receiver iteration, a list of good candidate bit sequences (and their corresponding metrics) is generated prior to the computation of the extrinsic information, with the aid of a breadth-first tree search algorithm known as the M-algorithm [14–16]. A detailed description of the basic ITS detection scheme follows in Section 3.1. For high-order QAM constellations, the complexity of the ITS detector can be reduced further by using a multilevel bit mapping. This is the subject of Section 3.2.

3.1 Basic scheme

The squared vector norm in (2.6) can be rewritten as

$$\|\mathbf{y} - \mathbf{H}\mathbf{s}\|^2 = (\mathbf{s} - \hat{\mathbf{s}})^\dagger \mathbf{H}^\dagger \mathbf{H} (\mathbf{s} - \hat{\mathbf{s}}), \tag{3.1}$$

where $\hat{\mathbf{s}} = [\hat{s}_1, \cdots, \hat{s}_{N_t}]^T = (\mathbf{H}^\dagger\mathbf{H})^{-1}\mathbf{H}^\dagger\mathbf{y}$ is the unconstrained maximum-likelihood (ML) solution [3]. The superscript $\dagger$ denotes conjugate transpose. Because $\mathbf{H}^\dagger\mathbf{H}$ is Hermitian and positive-definite, it has a Cholesky decomposition $\mathbf{H}^\dagger\mathbf{H} = \mathbf{L}^\dagger\mathbf{L}$, in which $\mathbf{L} = [l_{ij}]$ is an $N_t \times N_t$ lower triangular matrix with real, positive diagonal entries. The metric $\mu(\mathbf{s})$ can now be rewritten as

$$\mu(\mathbf{s}) = -\frac{1}{\sigma_n^2} \sum_{i=1}^{N_t} \left| l_{ii}(s_i - \hat{s}_i) + \sum_{j=1}^{i-1} l_{ij}(s_j - \hat{s}_j) \right|^2 + \sum_{i=1}^{N_t} \sum_{j \in \mathbb{J}_i} L_A(x_{i,j}). \tag{3.2}$$

This metric can be computed in a symbol-by-symbol manner, starting with the first symbol s_1 and proceeding to s_{N_t}, by exploiting the relationships

$$\begin{aligned}
\mu_1 &= -\frac{1}{\sigma_n^2} |l_{11}(s_1 - \hat{s}_1)|^2 + \sum_{j \in \mathbb{J}_1} L_A(x_{1,j}) \\
\mu_i &= \mu_{i-1} - \frac{1}{\sigma_n^2} \left| l_{ii}(s_i - \hat{s}_i) + \sum_{j=1}^{i-1} l_{ij}(s_j - \hat{s}_j) \right|^2 + \sum_{j \in \mathbb{J}_i} L_A(x_{i,j}), \quad i = 2, \cdots, N_t \\
\mu(\mathbf{s}) &= \mu_{N_t}.
\end{aligned} \tag{3.3}$$

This property, which hinges on the lower triangular structure of $\mathbf{L}$, is used in the ITS scheme to generate a list of good candidate bit sequences, or candidate list. This is described next.

A symbol vector $\mathbf{s}$ consists of N_t symbols, each chosen from an alphabet of size 2^{M_c}. The set of all possible symbol vectors can therefore be represented by a tree structure of depth N_t, having a single symbol on each branch and 2^{M_c} branches out of each node, as illustrated in Fig. 3.1. Associated with each path within the tree are a sequence of symbols $s_1, \cdots, s_d$ and a metric μ_d, where $d \leq N_t$ indicates the symbol depth of the path. Every possible symbol vector corresponds to a path to the maximum symbol depth, N_t, and has a total metric $\mu(\mathbf{s}) = \mu_{N_t}$.

The ITS detector uses a breadth-first tree search algorithm known as the M-algorithm [14] to search for the best paths through the tree. To this end, at each symbol depth smaller than N_t, the

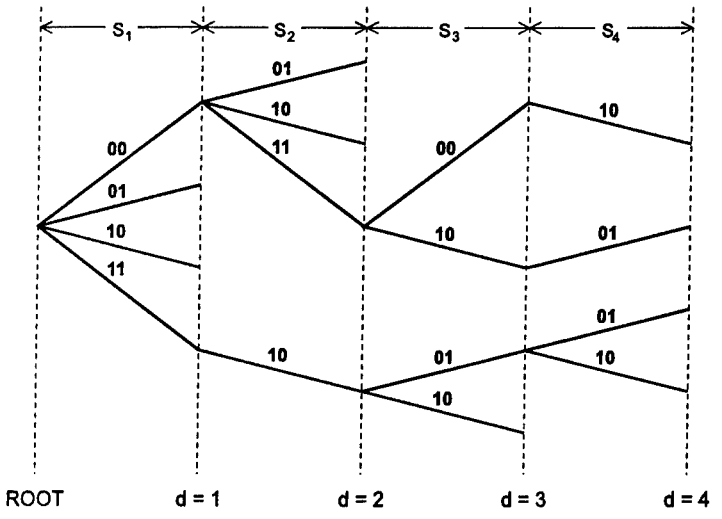

Figure 3.1. Example of a sequential tree search, for $N_t = 4$, $M_c = 2$. At each symbol depth, the best $M = 4$ paths are retained. Deleted paths are not shown.

algorithm keeps a list of the best M paths found thus far and their metrics, and moves forward by extending each of these paths to form $M \cdot 2^{M_c}$ new paths. Metrics are then updated according to (3.3), and the $M(2^{M_c} - 1)$ worst paths are deleted. The heart of the M-algorithm is a sorting procedure which deletes these paths. An attractive implementation of this procedure is the heapsort algorithm [17]. Heapsort is particularly suitable if only a partial ordering is desired, as is the case here. Furthermore, its complexity is guaranteed to be $\mathcal{O}(n \log n)$, n being the number of input data, and is almost independent of the distribution of the input data[1]. This is a favourable property with regard to practical implementation.

After having generated the candidate list, denoted here by $\mathbb{L}$, the ITS detector computes an approximation of (2.4) as

$$L_E(x_{n,k}) = \log \frac{\sum\limits_{\mathbf{x} \in (\mathbb{L} \cap \mathbb{X}_{n,k}^{+1})} \exp\ \mu(\mathbf{s})}{\sum\limits_{\mathbf{x} \in (\mathbb{L} \cap \mathbb{X}_{n,k}^{-1})} \exp\ \mu(\mathbf{s})} - L_A(x_{n,k}). \tag{3.4}$$

In practice, the log-sum over exponential functions, which is a relatively complex operation, can be approximated by

$$\log \sum_j \exp\ \mu_j \approx \max_j \mu_j \tag{3.5}$$

with little performance degradation. This is referred to as the max-log approximation [18].

Theoretically, the performance of the ITS detector is identical to that of the MAP detector only for the maximum possible list size, i.e., for $M = 2^{N_t M_c}$. In practice, however, near-optimum performance can often be achieved when M is only a small fraction of $2^{N_t M_c}$. The efficiency of the ITS detector in approaching MAP performance depends on the correlation between the columns of the channel matrix $\mathbf{H}$, which is identical to the correlation between the columns of $\mathbf{L}$ because $\mathbf{H}^\dagger \mathbf{H} = \mathbf{L}^\dagger \mathbf{L}$. For example, if the columns of $\mathbf{H}$ are orthogonal, so that $\mathbf{L}$ is diagonal, the search

[1] Here and in the following, Landau's symbol $\mathcal{O}$, which suggests "order", is used to indicate that, for large n, the function $f(n) = \mathcal{O}(h(n))$ is proportional to $h(n)$.

over each symbol is independent of decisions made on previous symbols, and the M-algorithm is guaranteed to yield the M best candidate symbol vectors. In that extreme case, the performance of the ITS detector is near-optimum even for very small list sizes. In the other extreme, if $\mathbf{H}$ is fully correlated, $\mathbf{L}$ degenerates to a matrix whose elements are zero, except those in the bottom row. In that case, the metric $\mu(\mathbf{s})$ can no longer be computed in a symbol-by-symbol manner, as in (3.3), and near-optimum performance can only be achieved with very large list sizes, i.e., with a nearly exhaustive tree search.

Another consequence of the use of the M-algorithm instead of an exhaustive tree search is that there may be positions for which all bit sequences used in the LLR computation (3.4) have the same binary value. This possibility becomes increasingly likely for smaller list sizes, and is certain to occur if $M \leq N_t M_c$. In such a case, (3.4) cannot be evaluated because either $\mathbb{L} \cap \mathbb{X}_{n,k}^{+1}$ or $\mathbb{L} \cap \mathbb{X}_{n,k}^{-1}$ is empty. Instead, $L_E(x_{n,k})$ is then assigned a negative or positive clipping value, $\mp L_{E,\text{clip}}$, respectively. It was found that the choice of the clipping value can affect the performance of the iterative receiver. Ideally, $L_{E,\text{clip}}$ should be different for each channel bit $x_{n,k}$, as follows:

$$L_{E,\text{clip}} = \log \frac{\Pr\{x_{n,k} L_E(x_{n,k}) > 0\}}{1 - \Pr\{x_{n,k} L_E(x_{n,k}) > 0\}}, \tag{3.6}$$

where $\Pr\{x_{n,k} L_E(x_{n,k}) > 0\}$ represents the probability that the bit sequences in $\mathbb{L}$ contain the true binary value for $x_{n,k}$, i.e., that the decision to drop all bit sequences with a different binary value was correct. It can be shown that this clipping value maximizes the mutual information between $x_{n,k}$ and $L_E(x_{n,k})$, i.e.,

$$I\big(L_E(x_{n,k}); x_{n,k}\big) = 1 - E\big\{\log_2\big(1 + e^{-x_{n,k} L_E(x_{n,k})}\big)\big\}. \tag{3.7}$$

In practice, however, the exact value of $\Pr\{x_{n,k} L_E(x_{n,k}) > 0\}$, which is dependent on many factors including signal-to-noise ratio (SNR) and channel correlation, is unknown, and a fixed clipping value is used. A constant clipping value that is much lower than the optimum value for a given $\Pr\{x_{n,k} L_E(x_{n,k}) > 0\}$ causes the channel decoder to largely ignore the clipped detector output values, which degrades its error-correction effectiveness. A clipping value that is much higher than its optimum value, on the other hand, forces the channel decoder to assume that the clipped detector output values have the correct sign. In the case that this assumption is false, soft decisions on other bits must be compromised in order to meet the code constraints, leading to error propagation. This performance degradation for relatively small or large clipping values is illustrated quantitatively in Fig. 3.2, which shows plots of the mutual information between $x_{n,k}$ and the clipped detector output $L_E(x_{n,k})$, versus the clipping value $L_{E,\text{clip}}$, for different values of $\Pr\{x_{n,k} L_E(x_{n,k}) > 0\}$. It is seen that the maximum amount of information contained in the clipped detector output values is relatively small for clipping values smaller than approximately 3. The mutual information also decreases for clipping values larger than approximately 2, but this effect is limited to lower values of $\Pr\{x_{n,k} L_E(x_{n,k}) > 0\}$. A reasonable balance can be found at intermediate clipping values, and good results were obtained with $L_{E,\text{clip}} = 3$, as can be seen in Sections 3.5 and 4.

The complexity per bit of the ITS detector is dominated by the metric update computation in (3.3) if N_t is large enough, and is therefore $\mathcal{O}(N_t)$. Because the number of metric updates to be computed at each symbol depth in the tree search is $M \cdot 2^{M_c}$, the complexity per bit depends on the signal constellation size as $\mathcal{O}(2^{M_c}/M_c)$.

3.2 Extension for multilevel bit mappings

The complexity per bit of the ITS detector can be made nearly independent of M_c with the aid of a special constellation mapping that is referred to herein as a multilevel bit mapping. By definition, a

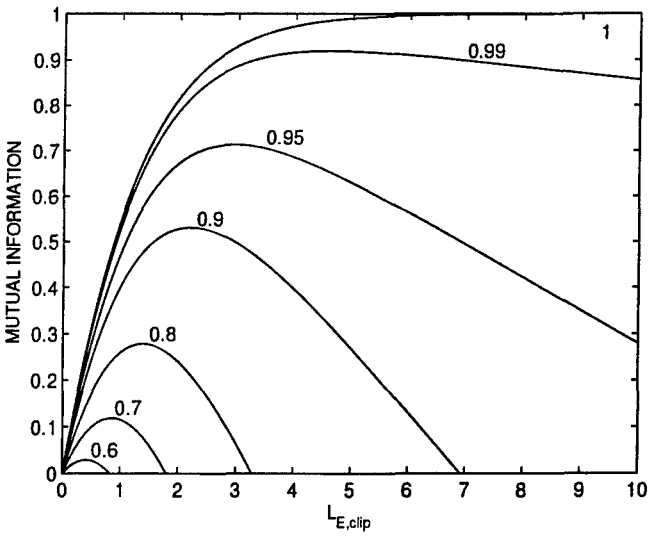

Figure 3.2. Mutual information $I(L_E(x_{n,k}); x_{n,k})$ vs. clipping value $L_{E,\text{clip}}$, for the values of $\Pr\{x_{n,k} L_E(x_{n,k}) > 0\}$ indicated.

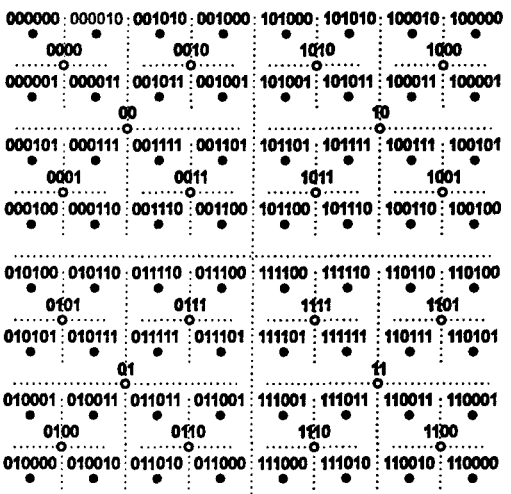

Figure 3.3. Example of a set of QAM signal constellations with a multilevel Gray bit mapping. 64-QAM ("level 3") signal points are represented by black dots. Associated 16-QAM ("level 2") and QPSK ("level 1") constellations are indicated by gray and white signal points, respectively.

QAM signal constellation with a multilevel bit mapping has the property that it can be partitioned into four equal subsets such that (a) the maximum Euclidean distance between the signal points in each subset is minimized, (b) each subset can be uniquely identified by the first two bits of its signal points, and (c) the remaining $M_c - 2$ bits of each subset again form a multilevel bit mapping. An example of a set of QAM signal constellations with a multilevel Gray bit mapping is given in Fig. 3.3, with intersecting dotted lines separating the subsets at each level. This figure also shows that, if the location of a higher-order, say 64-QAM signal point s is to be determined but only its first $2l < M_c$ bits are known, the best estimate is formed by the corresponding "intermediate" signal point at level l, denoted here by $s^{(l)}$. Subsequent pairs of bits refine this estimate, until all M_c bits are known.

The use of a multilevel bit mapping makes it possible to perform the tree search in steps of two bits, so that the number of branches emanating from each node is four, regardless of the modulation order. This is illustrated in Fig. 3.4, which shows an example of a search over a 64-QAM signal constellation at an arbitrary symbol depth of the tree search, for $M = 4$. At the left-hand side of the tree section shown, the path list contains the best M symbol sequences found before considering the current symbol. At the tree position marked "level 1", each of these paths is extended according to the four possible values of the first pair of bits in the current symbol, using the QPSK (4-QAM) constellation in Fig. 3.3. The corresponding metrics are then calculated, and the best M paths are retained. Likewise, at the position marked "level 2", all paths retained at the previous level are extended according to the four possible values of the subsequent bit pair, using the 16-QAM constellation in Fig. 3.3. Again, the corresponding metrics are calculated, and all but the best M paths are eliminated. Thus, the search over the current symbol constellation continues until the maximum level $l = M_c/2$ is reached. This modified ITS scheme will be referred to in the remainder of the report as multilevel mapping ITS (MLM-ITS).

Denoting the metric corresponding to level l of symbol depth d by $\mu_d^{(l)}$, the metric update relations for the MLM-ITS scheme can be written as

$$
\begin{aligned}
\mu_1^{(1)} &= -\frac{1}{\sigma_n^2}\left|l_{11}(s_1^{(1)} - \hat{s}_1)\right|^2 + \sum_{j \in \mathbb{J}_1^{(1)}} L_A(x_{1,j}) \\
\mu_i^{(l)} &= \mu_i^{(l-1)} + \frac{1}{\sigma_n^2}\left|l_{ii}(s_i^{(l-1)} - \hat{s}_i) + \sum_{j=1}^{i-1} l_{ij}(s_j - \hat{s}_j)\right|^2 \\
&\quad - \frac{1}{\sigma_n^2}\left|l_{ii}(s_i^{(l)} - \hat{s}_i) + \sum_{j=1}^{i-1} l_{ij}(s_j - \hat{s}_j)\right|^2 + \sum_{j \in \mathbb{J}_i^{(l)}} L_A(x_{i,j}), \\
&\qquad\qquad i = 1, \cdots, N_t, \quad l = 2, \cdots, M_c/2 \\
\mu_i^{(1)} &= \mu_{i-1}^{(M_c/2)} - \frac{1}{\sigma_n^2}\left|l_{ii}(s_i^{(1)} - \hat{s}_i) + \sum_{j=1}^{i-1} l_{ij}(s_j - \hat{s}_j)\right|^2 + \sum_{j \in \mathbb{J}_i^{(1)}} L_A(x_{i,j}), \\
&\qquad\qquad i = 2, \cdots, N_t \\
\mu(\mathbf{s}) &= \mu_{N_t}^{(M_c/2)},
\end{aligned}
\tag{3.8}
$$

in which

$$
\mathbb{J}_i^{(l)} = \left\{ j \,\middle|\, j \in \{2l-1, 2l\} \text{ and } x_{i,j} = +1 \right\}. \tag{3.9}
$$

The complexity per bit of MLM-ITS is still $\mathcal{O}(N_t)$, but is nearly independent of the constellation size, which is a major improvement over the basic ITS scheme. As will be shown in Section 3.5, this complexity reduction does not affect the performance of the detector.

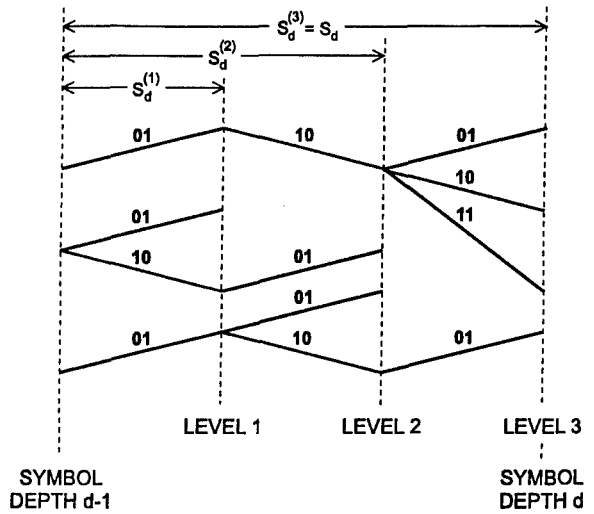

Figure 3.4. Example of a sequential tree search over a 64-QAM constellation with a multilevel bit mapping. At each level, the best $M = 4$ paths are retained. Deleted paths are not shown.

3.3 Comparison to BLAST

Some similarity exists between ITS detection and the non-iterative BLAST nulling/cancelling detection algorithm described in [19, 20]. In both schemes, the channel matrix is effectively transformed to a triangular form, such that the detection of any given symbol, say s_n, is only affected by the interference from previous symbols $s_1, \cdots, s_{n-1}$ (nulling). However, whereas the BLAST scheme immediately makes a hard decision on s_n and subtracts the detected symbol from the received signal vector (cancelling), the ITS detector retains and cancels several possible realizations of s_n. A hard decision is possibly forced at a later stage of the tree search, when, due to the limited list size, all candidate symbol vectors with a different realization of s_n are dropped from the candidate list. Because it is able to defer hard decisions until more symbols have been processed, the ITS detector effectively detects multiple symbols jointly, and is therefore less prone to error propagation than BLAST. Also, its performance is considerably less sensitive to the order in which the symbols are detected; simulations have shown that the gain in ITS performance due to optimal detection ordering, proposed in [20], would be 0.5 dB or less for the scenarios considered in the following sections. For a list size of one, the two schemes are basically identical, although BLAST does not accept soft input information and requires the channel code blocks to be organized in a specific (diagonally or vertically layered) manner, whereas ITS detection permits arbitrary code block organization.

3.4 Computational complexity

The complexities of the basic ITS and MLM-ITS detection schemes were analyzed by measuring the execution times of their algorithm components. Since they constitute the bulk of the total complexity, only the components that must be executed for every symbol were considered. These include the metric update defined by (3.3) and (3.8), respectively, as well as the heapsort sorting routine and the LLR computation (3.4), approximated by the max-log approximation. The complexity associated with the computation of the ML symbol estimate $\hat{s}_n$ is negligible, and was therefore not considered.

In the complexity analysis, identical assumptions were made with regard to the implementation of both detection schemes. Care was taken to code all algorithm components efficiently, and the

resulting C source code was compiler-optimized for and run on the same Intel Pentium III-based platform. The MIMO configurations considered were 4×4 and 8×8, the modulation formats were QPSK (4-QAM), 16-QAM and 64-QAM, and the ITS list size, M, was varied from 8 to 64. All measured complexities were normalized to the total complexity of the basic ITS detector for 4×4 QPSK with $M = 8$. Note that, for both schemes, the complexity per bit is proportional to the number of iterations in the detector/decoder loop.

Table 3.1 shows the normalized measured complexity per bit of basic ITS and MLM-ITS. It is seen that, except for QPSK modulation, the complexity of MLM-ITS is significantly lower than that of basic ITS. For example, for 8×8 64-QAM, MLM-ITS is approximately six times faster than basic ITS. This difference is due mainly to the complexity reduction of the metric update, although the complexity of the heapsort routine is also lower, because the number of paths to be sorted in the tree search is reduced from $M \cdot 2^{M_c}/M_c$ to $2M$ per bit. For both ITS schemes, the complexity of the metric update is proportional to M, while the heapsort complexity grows somewhat faster than linearly with M, as expected from the discussion in Section 3.1. The complexity per bit of the metric update increases linearly with N_t, as expected, but this dependency is only weak. This is especially true for basic ITS with large signal constellations, where the metric update complexity is dominated by operations that are independent of N_t. Note that the ITS complexity does not depend on N_r. For each of the two ITS schemes, the overall complexity per bit is approximately proportional to M, and increases only slightly with increasing N_t. The total complexity per bit of basic ITS is proportional to the signal constellation size, whereas that of MLM-ITS is nearly independent of M_c.

It has been shown in [2] that the performance reduction of the modified ITS scheme (MLM-ITS) relative to the basic ITS scheme does not affect performance, i.e., the performance difference between basic ITS and MLM-ITS is negligible. This implies that MLM-ITS should be used instead of basic ITS wherever applicable. For this reason, the performance results shown in the remainder of this report were all generated using the MLM-ITS detector.

3.5 Performance under ideal channel conditions

This section presents error performance results obtained from computer simulations of an iterative MIMO receiver employing the MLM-ITS detector, under ideal channel conditions, i.e., perfect channel estimation, and rapid and spatially uncorrelated fading. The effects of non-perfect channel estimation, fading correlation and slow fading are investigated in the next chapter.

The simulation results presented in the remainder of this report were generated for a 4×4 MIMO configuration with QPSK, 16-QAM and 64-QAM modulation, with the multilevel Gray mapping shown in Fig. 3.3. The channel code is a turbo code of rate 1/2 and memory 2, with feedforward and feedback generators 5 and 7 (octal), respectively. Frames of 9216 information bits are fed to the channel encoder, and subsequently transmitted over a block fading channel, represented by the propagation matrix $\mathbf{H}$. In this section, the elements of $\mathbf{H}$ are samples of independent, complex-valued, zero-mean Gaussian processes, and thus model a rich scattering (Rayleigh) MIMO channel. The channel remains constant over $N_t M_c/2$ information bits, or $N_t M_c$ code bits, and changes to a new, statistically independent realization between these blocks. All interleavers are pseudorandom, and, as theory predicts that bad interleavers are rare if the frame size is large, no attempt was made to optimize their design. The number of iterations in the turbo decoder is eight, and that in the detector/decoder loop is four, unless noted otherwise. Except for some of the results in Fig. 3.7, the detector output is computed using the max-log approximation (3.5); no approximations are made in the turbo channel decoder. The clipping value $L_{E,\text{clip}}$ is equal to 3, as discussed in Section 3.1. The list size M is varied between 8 and 64. The average SNR at each receive antenna is denoted by

Table 3.1. Normalized measured complexity per bit of basic ITS and MLM-ITS detection. Entries contain basic ITS and MLM-ITS complexities, respectively, separated by slashes.

	METRIC UPDATE	HEAPSORT	LLR COMP.	TOTAL
4×4 QPSK, M = 8	0.6 / 0.6	0.3 / 0.3	0.1 / 0.1	1.0 / 1.0
4×4 QPSK, M = 16	1.2 / 1.2	0.7 / 0.7	0.2 / 0.2	2.1 / 2.1
4×4 QPSK, M = 32	2.4 / 2.4	1.6 / 1.6	0.3 / 0.3	4.3 / 4.3
4×4 QPSK, M = 64	4.8 / 4.8	3.4 / 3.4	0.5 / 0.5	8.7 / 8.7
4×4 16-QAM, M = 8	1.5 / 0.6	0.5 / 0.3	0.1 / 0.1	2.1 / 1.1
4×4 16-QAM, M = 16	3.1 / 1.3	1.0 / 0.7	0.2 / 0.2	4.3 / 2.1
4×4 16-QAM, M = 32	6.2 / 2.6	2.1 / 1.6	0.3 / 0.3	8.6 / 4.5
4×4 16-QAM, M = 64	12.5 / 5.2	4.2 / 3.4	0.5 / 0.5	17.3 / 9.0
4×4 64-QAM, M = 8	6.3 / 0.7	1.1 / 0.3	0.1 / 0.1	7.6 / 1.1
4×4 64-QAM, M = 16	12.7 / 1.3	2.3 / 0.7	0.2 / 0.2	15.1 / 2.2
4×4 64-QAM, M = 32	25.4 / 2.6	4.9 / 1.6	0.3 / 0.3	30.6 / 4.5
4×4 64-QAM, M = 64	50.9 / 5.2	10.1 / 3.4	0.5 / 0.5	61.5 / 9.1
8×8 QPSK, M = 8	0.7 / 0.7	0.3 / 0.3	0.1 / 0.1	1.1 / 1.1
8×8 QPSK, M = 16	1.5 / 1.5	0.7 / 0.7	0.2 / 0.2	2.3 / 2.3
8×8 QPSK, M = 32	2.9 / 2.9	1.6 / 1.6	0.3 / 0.3	4.8 / 4.8
8×8 QPSK, M = 64	5.8 / 5.8	3.4 / 3.4	0.5 / 0.5	9.8 / 9.8
8×8 16-QAM, M = 8	1.6 / 0.8	0.5 / 0.3	0.1 / 0.1	2.2 / 1.2
8×8 16-QAM, M = 16	3.2 / 1.5	1.0 / 0.7	0.2 / 0.2	4.4 / 2.4
8×8 16-QAM, M = 32	6.4 / 3.1	2.1 / 1.6	0.3 / 0.3	8.8 / 5.0
8×8 16-QAM, M = 64	12.9 / 6.1	4.2 / 3.4	0.5 / 0.5	17.7 / 10.1
8×8 64-QAM, M = 8	6.4 / 0.8	1.1 / 0.3	0.1 / 0.1	7.6 / 1.2
8×8 64-QAM, M = 16	12.8 / 1.5	2.3 / 0.7	0.2 / 0.2	15.3 / 2.4
8×8 64-QAM, M = 32	25.4 / 3.1	4.9 / 1.6	0.3 / 0.3	30.7 / 5.0
8×8 64-QAM, M = 64	51.0 / 6.1	10.1 / 3.4	0.5 / 0.5	61.8 / 10.1

Sum of partial complexities may not agree with total complexity due to independent rounding.

$E_s/N_0 = N_t \cdot \sigma_s^2/\sigma_n^2$, where $\sigma_s^2 = E\{|s_n|^2\}$ is the average power used on each transmit antenna.

The simulation results of Fig. 3.5(a) and (b) show the dependence of the MLM-ITS bit error performance on the number of iterations in the detector/decoder loop, for list sizes of $M = 8$ and 64, respectively. It can be seen that iterative MIMO systems have considerably improved performance relative to non-iterative systems, i.e., systems for which the number of iterations is one. Most of the gain achieved by iterating the receiver is obtained in the second iteration, and increasing the number of iterations further results in rapidly diminishing gains. For example, the performance gain that is achieved by increasing the number of iterations from 3 to 6 is smaller than 1 dB for all modulation formats considered in Fig. 3.5. This observation is valid both for $M = 8$ and $M = 64$, and is also in agreement with results reported in [5] and [4, 6], discussed in Section 2.2, even though the latter were obtained with different detection and channel coding schemes than the ones considered here. This suggests that the convergence behaviour is not very highly dependent on the type of detector or, in the case of MLM-ITS detection, its list size. Instead, "external" factors such as interleaver depth appear to be more important [12]. The complexity of iterative receivers is proportional to the number of iterations. Based on the results of Fig. 3.5, it can be concluded that a good balance between performance and complexity can be achieved with 3-4 iterations.

The bit error performance of MLM-ITS detection as a function of the list size M is shown in Fig. 3.6. As expected, performance improves if the list size M is increased, in this case from 8 to 64. However, the improvement becomes smaller as the ratio between M and the maximum list size, $2^{N_t M_c}$, increases. For example, the performance improvement due to increasing M from 8 to 64 is approximately 2 dB for 4×4 64-QAM ($2^{N_t M_c} = 2 \times 10^7$), but negligible for 4×4 QPSK ($2^{N_t M_c} = 256$).

The potential performance degradation due to the max-log approximation (3.5) in the computation of the detector output (3.4) was also investigated. Fig. 3.7 shows the bit error performance obtained using the true sum of exponentials and the max-log approximation. Based on the very small performance difference observed in Fig. 3.7, it can be concluded that the max-log approximation should be used where applicable, because it eliminates most of the complexity involved in evaluating the detector output, at almost negligible performance loss. The fact that the detector using the true sum of exponentials performs slightly worse than the detector using the max-log approximation may be a result of numerical instabilities, which are known to be a problem in the evaluation of (3.4).

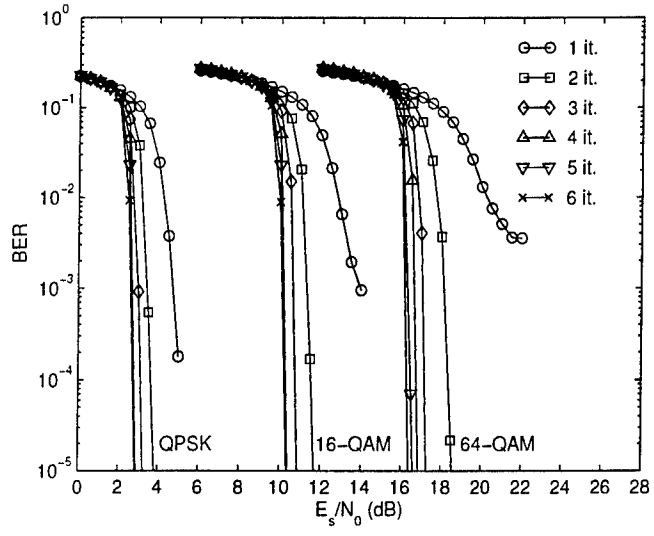

(a)

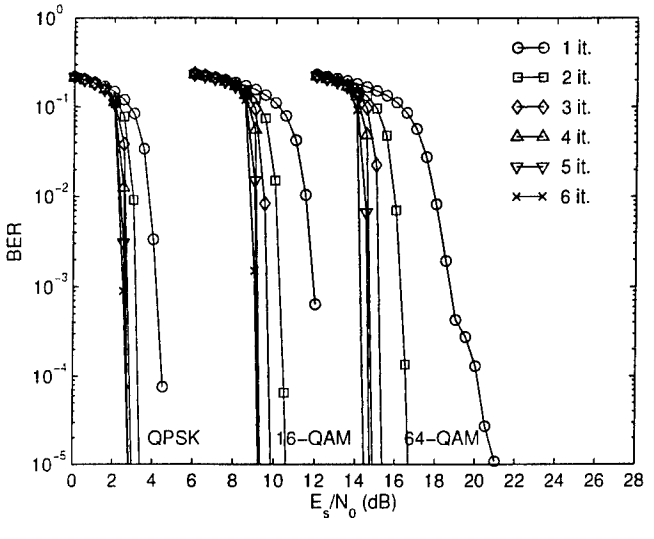

(b)

Figure 3.5. Error performance of a 4×4 ST-BICM MIMO system employing the MLM-ITS detector, for different numbers of iterations in the detector/decoder loop, and for (a) $M = 8$, and (b) $M = 64$. Channel code is a turbo code of rate 1/2 and memory 2.

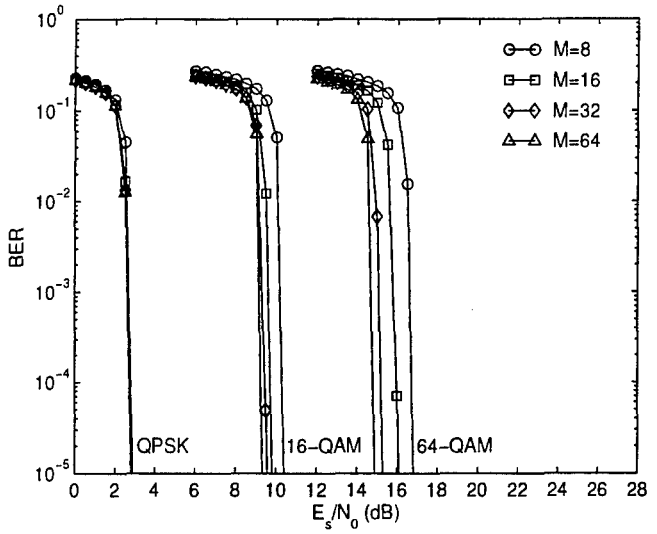

Figure 3.6. Error performance of a 4×4 ST-BICM MIMO system employing the MLM-ITS detector, for different values of the list size M. Number of iterations in the detector/decoder loop is four. Channel code is a turbo code with rate 1/2 and memory 2.

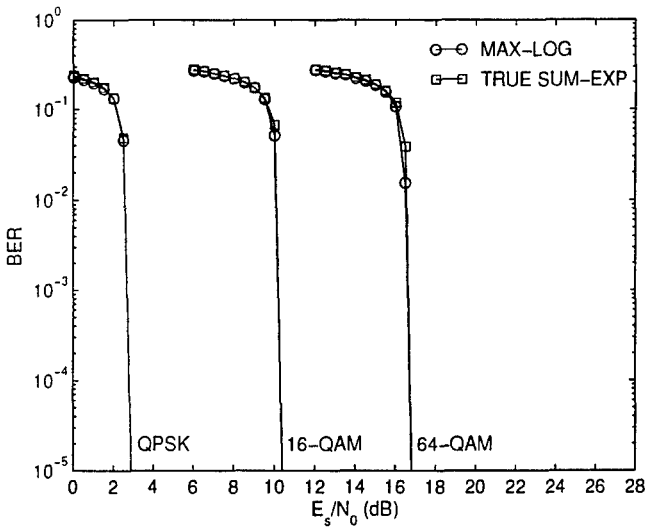

Figure 3.7. Error performance of a 4×4 ST-BICM MIMO system employing the MLM-ITS detector, with and without using the max-log approximation in the computation of the detector output. Number of iterations in the detector/decoder loop is four. Channel code is a turbo code with rate 1/2 and memory 2.

4 Issues regarding implementation in real-world MIMO systems

4.1 Channel estimation

So far in this report, it has been assumed that the channel matrix $\mathbf{H}$ and the noise variance σ_n^2 are known perfectly at the receiver. In practice, such channel state information is not available, and $\mathbf{H}$ and σ_n^2 must be estimated from the received signal vector $\mathbf{y}$, based on knowledge of the transmitted symbol vector $\mathbf{s}$. The most straightforward channel estimation method is channel training, which involves the transmission of known, or pilot symbol vectors for a certain fraction of the frame duration, called the training overhead factor. Because the pilot symbol vectors themselves do not convey any information, channel training reduces the overall data throughput. Another channel estimation method, which does not affect throughput, is to exploit information about the transmitted signal vector produced by the detector or the channel decoder. This method is commonly referred to as decision feedback, or soft decision feedback if soft decisions are involved, which is usually the case in iterative receivers. The optimum MIMO channel estimation scheme, in the sense that it maximizes the likelihood of the received signal vector $\mathbf{y}$ given the transmitted symbol vector $\mathbf{s}$, is defined by

$$\hat{\mathbf{H}} = \hat{\mathbf{R}}_{ys}\hat{\mathbf{R}}_s^{-1}, \tag{4.1}$$

where $\hat{\mathbf{R}}_{ys}$ and $\hat{\mathbf{R}}_s$ denote estimates of the correlation matrices $\mathbf{R}_{ys} = E\{\mathbf{y}\mathbf{s}^\dagger\}$ and $\mathbf{R}_s = E\{\mathbf{s}\mathbf{s}^\dagger\}$. The estimation of $\mathbf{R}_{ys}$ and $\mathbf{R}_s$, and hence $\mathbf{H}$, by means of finite-length channel training and soft decision feedback, respectively, is discussed in the next sections. The estimation of σ_n^2 is addressed in Section 4.1.3.

4.1.1 Channel training

If a finite number, N_p, of pilot symbol vectors, denoted by $\mathbf{s}_{p,i}$, $i = 1, \cdots, N_p$, is available for channel estimation, $\mathbf{R}_{ys}$ and $\mathbf{R}_s$ are estimated as follows:

$$\begin{aligned} \hat{\mathbf{R}}_{ys} &= \frac{1}{N_p}\mathbf{y} \cdot \sum_{i=1}^{N_p} \mathbf{s}_{p,i}^\dagger \\ \hat{\mathbf{R}}_s &= \frac{1}{N_p}\sum_{i=1}^{N_p} \mathbf{s}_{p,i}\mathbf{s}_{p,i}^\dagger. \end{aligned} \tag{4.2}$$

It is noted that N_p must be at least equal to the number of transmit antennas in order for the matrix inversion in (4.1) to exist. It has been shown in [21] that, to minimize the mean squared channel estimation error, the training symbol vectors must be orthogonal and of equal power, so that $\hat{\mathbf{R}}_s$ is diagonal with equal diagonal elements. It can be shown that the channel estimation accuracy, expressed in terms of the mean SNR per element of $\hat{\mathbf{H}}$, can then be written as

$$\frac{E\{(\hat{h}_{ij} - h_{ij})(\hat{h}_{ij} - h_{ij})^*\}}{E\{h_{ij}h_{ij}^*\}} = \frac{N_p}{N_t} \cdot \frac{E_s}{N_0}, \tag{4.3}$$

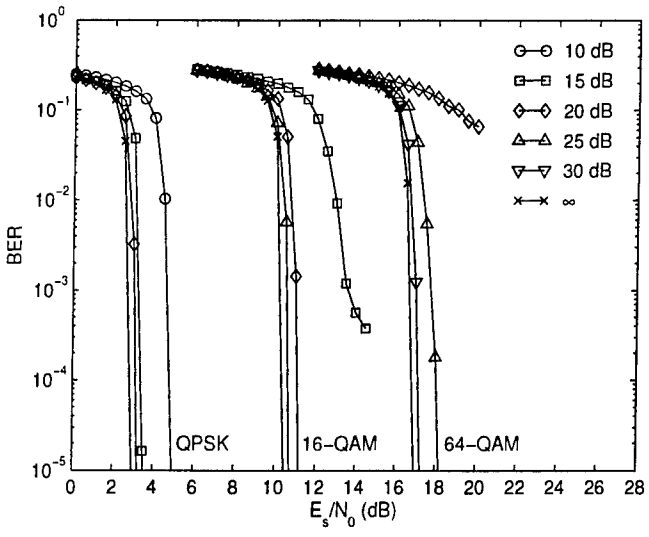

Figure 4.1. Error performance of a 4 × 4 ST-BICM MIMO system employing the MLM-ITS detector with $M = 8$, for different channel estimation accuracies. Number of iterations in the detector/decoder loop is four. Channel code is a turbo code with rate 1/2 and memory 2.

where h_{ij} and $\hat{h}_{ij}$ denote the (i, j)th element of $\mathbf{H}$ and $\hat{\mathbf{H}}$, respectively, and E_s/N_0 is the SNR at each receive antenna, as previously. It follows from Eq. (4.3) that, if $N_p = N_t$, the mean SNR of the elements of $\mathbf{H}$ is equal to E_s/N_0. If better channel estimation accuracy is required, the number of pilot symbol vectors must be increased. Alternatively, the transmit power in the training interval could be increased. However, the benefit of this option is limited, because the payload power would then have to be reduced in order to keep the overall transmit power constant. An information-theoretic analysis in [21] has shown that, under typical conditions, the capacity gain resulting from the optimization of training and payload powers is only 5–10%. Also, this approach causes some difficulties concerning the implementation of the transmitter front end, most notably a loss in power efficiency due to the increased peak-to-average power ratio.

In order to evaluate the sensitivity of the MLM-ITS detector to channel estimation errors, computer simulations were performed in which the detector was provided with a copy of $\mathbf{H}$ whose elements were corrupted by additive complex Gaussian noise. The average SNR of the matrix elements is used as a measure for the channel estimation accuracy. Simulation results for a 4×4 MIMO configuration with $M = 8$ are shown in Fig. 4.1. All other parameters were kept the same as in Section 3.5. It is seen that performance degradation is almost negligible (< 1 dB) if the channel estimation SNR is at least 10 dB higher than the E_s/N_0 required for "error-free" transmission (BER $< 10^{-5}$) with perfect channel estimation. For example, for 4×4 64-QAM and perfect channel knowledge, error-free performance is achieved at values of E_s/N_0 higher than approximately 17 dB. Performance degradation is approximately 1 dB for a channel estimation SNR of 25 dB, which is 8 dB above E_s/N_0, and becomes smaller if the channel estimation accuracy is improved further. For channel estimation SNRs lower than approximately 10 dB above E_s/N_0, performance degradation increases rapidly. Similar observations can be made for the other curves in Fig. 4.1. From these results it can be concluded that, if the channel estimation scheme relies on training only, the number of pilot symbol vectors must be at least ten times higher than the number of transmit antennas for negligible performance degradation, i.e., $N_p/N_t > 10$.

In order to conserve throughput, it is generally desirable to limit the training overhead factor to

approximately 10% or less, which can be achieved only if the training period is at least an order of magnitude shorter than the channel coherence time, which is denoted by T_c and will be discussed in more detail in Section 4.3. It thus follows that the symbol vector transmission rate must be at least two orders of magnitude higher than the ratio N_t/T_c, i.e., the coded bit rate must be greater than approximately $100N_t^2M_c/T_c$. The coherence time depends strongly on the propagation environment, and can vary from approximately 1 ms for high-speed mobile applications to approximately 100 ms for indoor applications. For example, a 4×4 64-QAM MIMO system designed to operate in an indoor environment with $T_c = 100$ ms must have a coded bit rate higher than approximately 100 kbps in order for performance loss due to imperfect channel estimation to be negligible. If lower data rates are desired, soft-decision feedback can be employed to enhance channel estimation while preserving information throughput, as discussed in the next section.

4.1.2 Soft decision feedback

The training overhead required for accurate channel estimation can be reduced by exploiting the soft decisions on the transmitted data produced by the detector or the channel decoder. Such soft decision feedback schemes have, for example, been proposed in [6, 7, 22]. Typically, in these schemes an initial channel estimate is produced with the aid of a relatively small number of pilot symbol vectors. In addition, LLR values pertaining to the code bits transmitted during the payload interval are used to generate soft estimates, $\tilde{\mathbf{s}}$, of the data symbol vectors. These soft estimates are then used to improve the estimates of $\mathbf{R}_{ys}$ and $\mathbf{R}_s$ required to compute $\hat{\mathbf{H}}$. In iterative receivers, the channel estimation accuracy tends to improve in later iterations, as the soft decisions produced by the detector and the decoder become more reliable. It was reported in [6] that, under certain conditions including the use of QPSK modulation and convolutional coding, such an iterative channel estimation scheme can achieve almost the same error performance as if perfect channel knowledge were available, although more detector/decoder iterations are required. The question of whether this conclusion is also valid for MIMO systems with high-order QAM modulation, different coding schemes, arbitrary numbers of antennas, etc., is a topic for further research. Another question that is still open is whether it is better to use soft feedback from the detector or from the channel decoder. While the soft information produced by the detector tends to be less reliable than that from the decoder, it becomes available earlier in the iterative process, and can be used to improve the channel estimate, and hence detection reliability, in the same iteration as it was generated. The latter factor is expected to outweigh the former.

A shortcoming of the soft decision feedback channel estimation technique outlined above is that it does not perform well if no reliable soft decision feedback is available, so that $\tilde{\mathbf{s}}$ is a poor estimate of the true symbol vector. In that case, taking into account soft decision feedback actually degrades the channel estimate obtained with channel training only. This problem can be alleviated by only taking into account the soft estimates of symbol vectors whose LLR values all exceed a certain magnitude threshold, as proposed in [6]. However, because this method typically ignores many LLR values with moderate to high magnitudes, it does not exploit the full potential of soft decision feedback.

A possibly more efficient approach to utilizing soft information for channel estimation, which is quite natural to the MLM-ITS detection scheme, is to update the estimates of the correlation matrices $\mathbf{R}_{ys}$ and $\mathbf{R}_s$, and hence of $\mathbf{H}$, with the aid of a list of symbol vectors and their estimated likelihoods of being the true symbol vector. As discussed in Section 3.1, a list of bit sequences likely to have been transmitted, referred to as the candidate list and denoted by $\mathbb{L}$, is automatically generated by the MLM-ITS detector in every iteration. It is straightforward to compute an estimate of the likelihood of a candidate symbol vector from the list of metrics associated with $\mathbb{L}$. Denoting

the likelihood of the symbol vector $\mathbf{s}$, and hence the corresponding bit sequence $\mathbf{x}$, by $p(\mathbf{s})$, $\hat{\mathbf{R}}_{ys}$ and $\hat{\mathbf{R}}_s$ can be updated as follows:

$$\begin{aligned}
\hat{\mathbf{R}}_{ys} &\leftarrow \frac{N_s}{N_s+1}\hat{\mathbf{R}}_{ys} + \frac{1}{N_s+1}\mathbf{y}\cdot\sum_{\mathbf{x}\in\mathbb{L}} p(\mathbf{s})\mathbf{s}^\dagger \\
\hat{\mathbf{R}}_s &\leftarrow \frac{N_s}{N_s+1}\hat{\mathbf{R}}_s + \frac{1}{N_s+1}\sum_{\mathbf{x}\in\mathbb{L}} p(\mathbf{s})\mathbf{s}\mathbf{s}^\dagger \\
N_s &\leftarrow N_s+1,
\end{aligned} \tag{4.4}$$

where N_s is the number of symbol periods over which $\hat{\mathbf{R}}_{ys}$ and $\hat{\mathbf{R}}_s$ are computed, including the pilot symbol intervals. In contrast to the iterative channel estimation schemes proposed in [6, 7, 22], soft decision feedback based on the correlation matrix update equations (4.4) does not degrade the initial channel estimate even if no reliable soft information is available, because the likelihoods $p(\mathbf{s})$ are small in that case. A more detailed investigation of this approach, including an evaluation of its performance and computational complexity, is a topic for future research.

Other issues that need to be addressed include the complexity associated with the direct matrix inversion in the ML channel estimate (4.1), and the capability to track channel variations other than the abrupt changes hypothesized in the block fading channel model adopted herein. Although this model provides a tractable method to obtain insight into the effects of temporal channel variations on MIMO performance, it does not accurately represent the characteristics of real-world MIMO channels. Practical radio channels change with time continuously, which implies that their estimates will become increasingly unreliable, unless tracking between training intervals is performed. This also implies that channel information obtained in previous training intervals does not necessarily become irrelevant when the channel estimate is updated, but, if suitably weighted, can be used to enhance estimation accuracy [23]. Both issues can possibly be addressed by modifying the update equations (4.4) and approximating (4.1) using a gradient descent approach, thus avoiding a matrix inversion, as proposed in [24].

4.1.3 Noise variance estimation

In comparison to the estimation of the channel matrix $\mathbf{H}$, the estimation of the noise variance σ_n^2 is a minor problem, because it involves only a single parameter that is normally not rapidly varying. Because σ_n^2 is identical for each receive antenna, it can be written as

$$\sigma_n^2 = \frac{1}{N_r}\mathrm{tr}\, E\{\mathbf{n}\mathbf{n}^\dagger\} = \frac{1}{N_r}\mathrm{tr}\{\mathbf{R}_y - \mathbf{R}_{ys}\mathbf{H}^\dagger - \mathbf{H}\mathbf{R}_{ys}^\dagger + \mathbf{H}\mathbf{R}_s\mathbf{H}^\dagger\}, \tag{4.5}$$

where $\mathbf{R}_y = E\{\mathbf{y}\mathbf{y}^\dagger\}$, and $\mathbf{R}_{ys}$ and $\mathbf{R}_s$ were defined previously. Replacing all matrices on the right-hand side of (4.5) by their respective approximations, an estimate of σ_n^2 is obtained as

$$\hat{\sigma}_n^2 = \frac{1}{N_r}\mathrm{tr}\{\hat{\mathbf{R}}_y - \hat{\mathbf{R}}_{ys}\hat{\mathbf{R}}_s^{-1}\hat{\mathbf{R}}_{ys}^\dagger\}. \tag{4.6}$$

The matrix $\hat{\mathbf{R}}_y$ is computed by averaging $\mathbf{y}\mathbf{y}^\dagger$ over the same symbol intervals for which $\hat{\mathbf{R}}_{ys}$ and $\hat{\mathbf{R}}_s$ are computed.

4.2 Correlated fading

It is well known that, from a theoretical point of view, MIMO systems can achieve maximum capacity if the elements of the channel matrix $\mathbf{H}$ are uncorrelated, i.e., if $E\{h_{kl}h_{mn}^*\} = 0$ for $k \neq m$

and/or $l \neq n$. It is generally accepted that this channel condition occurs if the antenna elements at both the transmitter and the receiver are located sufficiently wide apart, and the physical propagation environment can be described as being "rich scattering". The latter term is used in a loose sense to indicate environments where many multipath components, comparable in terms of path gain but widely different with respect to their trajectories in space, are present. In real-world situations, the MIMO channel matrix is often correlated among its elements because one or more of these requirements are not fulfilled. This correlation, often referred to as fading correlation, has a detrimental effect on information-theoretic MIMO capacity, because it decreases the average number of usable spatial eigenmodes and their "gains", i.e., the eigenvalues of $\mathbf{H}\mathbf{H}^{\dagger}$ [25, 26]. In addition, as was discussed in Section 3.1, fading correlation degrades the performance of MLM-ITS detection relative to optimum, MAP detection.

In practical MIMO scenarios, the spacing between the elements in the transmit and receive arrays is usually much smaller than the distance between any pair of transmit and receive antennas, or from any antenna to the nearest scatterer. In such cases, the angles-of-arrival and amplitudes of the received signals from a single transmit antenna, and, therefore, the receive correlation, are approximately independent of the antenna's location within the transmit array. Likewise, the correlation between the transmitted signals measured at a single receive antenna is roughly independent of the antenna's location within the receive array. Under these assumptions, fading correlation can be separated into transmit and receive correlation, and characterized completely by the transmit and receive correlation matrices, $\mathbf{R}_t = E\{\mathbf{H}^{\dagger}\mathbf{H}\}$ and $\mathbf{R}_r = E\{\mathbf{H}\mathbf{H}^{\dagger}\}$, respectively. This is referred to as the Kronecker approximation in the MIMO literature [27]. As these matrices are dependent on the locations and other properties of scatterers surrounding the transmitter and receiver, they are generally different from one propagation environment to another, and must be determined by means of measurements. If relevant measurement data are not available, simple correlation models such as the uniform correlation model [28]

$$\mathbf{R}_t = N_r \cdot \begin{bmatrix} 1 & \rho_t & \dots & \rho_t \\ \rho_t & 1 & \dots & \rho_t \\ \vdots & \vdots & \ddots & \vdots \\ \rho_t & \rho_t & \dots & 1 \end{bmatrix}; \quad \mathbf{R}_r = N_t \cdot \begin{bmatrix} 1 & \rho_r & \dots & \rho_r \\ \rho_r & 1 & \dots & \rho_r \\ \vdots & \vdots & \ddots & \vdots \\ \rho_r & \rho_r & \dots & 1 \end{bmatrix}, \tag{4.7}$$

can be used. Here, the correlation coefficients ρ_t and ρ_r are restricted to be real-valued. Although such models do not accurately represent the MIMO channel characteristics encountered in real propagation environments, where the correlation coefficients are generally complex-valued and different from one another, they are useful for obtaining insight into the effects of fading correlation on the performance of MIMO systems.

A commonly used correlated Rayleigh fading MIMO channel model was proposed in [29, 30] and is given by

$$\mathbf{H} = \frac{1}{\sqrt{\mathrm{tr}\,\mathbf{R}_t}} \cdot \mathbf{R}_r^{1/2}\mathbf{G}\mathbf{R}_t^{1/2}, \tag{4.8}$$

where $\mathbf{G}$ is an $N_r \times N_t$ random matrix with independent, zero-mean, unit-variance complex entries drawn from a complex Gaussian distribution, and the matrix square root is defined such that $\mathbf{R}^{1/2}\mathbf{R}^{1/2} = \mathbf{R}$. The normalization factor in (4.8) ensures that the entries of $\mathbf{H}$ have unit variance. Note that the channel model above is only valid for real-valued correlation matrices. For simulation purposes it is further noted that, even if (4.8) were modified to be capable of dealing with complex-valued $\mathbf{R}_t$ and $\mathbf{R}_r$, one has to be careful that these correlation matrices must be positive-definite in order to be meaningful.

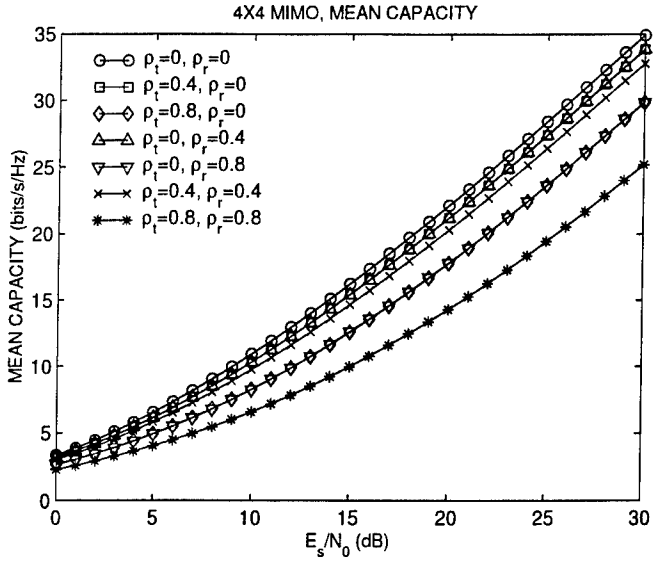

Figure 4.2. Mean MIMO channel capacity for various degrees of fading correlation. Channel code rate is 1/2.

Like the uniform correlation model described above, the channel model (4.8) is, in general, not an accurate representation of real-world MIMO channels, whose channel coefficients are not necessarily Rayleigh fading. Moreover, the properties of actual MIMO channels are not completely determined by the transmit and receive fading correlation. For example, it has been pointed out in [31] that the rank of the channel matrix can be consistently equal to one even when its entries are uncorrelated, i.e., when both $\mathbf{R}_t$ and $\mathbf{R}_r$ are diagonal. In such cases, spatial diversity is still available, but only a single spatial eigenmode is available for data transmission, as in single-antenna communications. This degenerate channel phenomenon is referred to as the keyhole (sometimes: pinhole) channel. Statistical channel models which model the fading of the entries of $\mathbf{H}$ as a product process of two complex Gaussian distributions include the correlated Rayleigh fading model (4.8) and the keyhole channel as special cases [32], and are therefore more general.

To investigate the effects of fading correlation on the performance of the MLM-ITS detector, a MIMO channel was simulated with the aid of (4.8) and the uniform correlation model. The transmit and receive correlation coefficients, ρ_t and ρ_r, were varied from 0 to 0.8. In order to provide a theoretical reference in terms of the performance loss associated with fading correlation, the mean MIMO channel capacity [25]

$$\overline{C} = E\left\{\log_2 \det\left(\mathbf{I} + \frac{E_s/N_0}{N_t}\mathbf{H}\mathbf{H}^\dagger\right)\right\} \tag{4.9}$$

was evaluated as a function of E_s/N_0 for the same values of ρ_t and ρ_r, and the results for a 4×4 MIMO configuration are shown in Fig. 4.2. These plots were obtained by averaging over 1000 independent realizations of $\mathbf{H}$, which is sufficient for a very good approximation of the true mean capacity. The information-theoretic performance loss relative to uncorrelated fading can be determined from this figure, and is given in Table 4.1. The values in this table were obtained assuming that the channel code rate is 1/2, and that the coded information is split into N_t equal-rate substreams, so that the overall information throughput is $N_t M_c/2$ bits/s/Hz. As discussed in Section 3.5, these assumptions are consistent with the simulations of the MLM-ITS detector presented in this report. It can be seen from Fig. 4.2 and Table 4.1 that the theoretical performance loss due to fading correlation is relatively small for correlation coefficients up to 0.4, but can become substantial for larger

Table 4.1. Information-theoretic performance loss, in dB relative to uncorrelated fading, for various degrees of fading correlation. Channel code rate is 1/2.

	4×4 QPSK	4×4 16-QAM	4×4 64-QAM
$\rho_t = 0.4, \rho_r = 0$	0.3	0.6	0.6
$\rho_t = 0, \rho_r = 0.4$	0.3	0.6	0.6
$\rho_t = 0.4, \rho_r = 0.4$	0.7	1.1	1.3
$\rho_t = 0.8, \rho_r = 0$	1.9	2.9	3.3
$\rho_t = 0, \rho_r = 0.8$	1.9	2.9	3.3
$\rho_t = 0.8, \rho_r = 0.8$	3.6	5.5	6.4

values. For example, the performance degradation of 4×4 64-QAM is 1.3 dB for $\rho_t = \rho_r = 0.4$, and 6.4 dB for $\rho_t = \rho_r = 0.8$. It is noted that the effects of transmit and receive correlation are identical. This is explained by the fact that the capacity formula (4.9) remains identical if the matrix product $\mathbf{H}\mathbf{H}^\dagger$, which represents fading correlation at the receiver, is replaced by $\mathbf{H}^\dagger\mathbf{H}$, which represents correlation at the transmitter.

The error performance of the MLM-ITS detector in a correlated Rayleigh fading channel was investigated by means of simulations. As previously, the fading correlation was modelled by the uniform correlation model, and ρ_t and ρ_r were varied from 0 to 0.8. The effects of transmit and receive correlation on system performance were found to be identical, as expected from theory, and will therefore not be addressed separately. Performance results for varying ρ_t and uncorrelated fading at the receiver are shown in Fig. 4.3. It is seen that the performance degradation is approximately 1 dB for $\rho_t = 0.4$, and in the range from 3.5 to 6 dB for $\rho_t = 0.8$. These values are considerably higher than the theoretical losses due to reduced channel capacity, listed in Table 4.1. The difference between the theoretical and actually observed performance loss can be attributed to the reduced efficiency of the MLM-ITS detector in approaching MAP performance as the channel matrix becomes more correlated, as discussed in Section 3.1. Results for fading correlation at both the transmitter and the receiver are shown in Fig. 4.4. As expected, performance loss in this case is higher than if the fading at either end of the channel is uncorrelated. Again, due to the reduced performance of the MLM-ITS detector relative to MAP detection, the observed losses are considerably higher than the theoretical values of Table 4.1.

It is clear from the above discussion that the degree of fading correlation has great impact on the performance of the MLM-ITS detector and, indeed, any MIMO detection scheme. Performance degradation of MLM-ITS detection with respect to the theoretical capacity bound is low for low fading correlation, but increases dramatically if correlation approaches its maximum. Correlation can sometimes be reduced by optimizing the transmitter and receiver locations such as to maximize the number and angular spread of the outgoing and incident multipath waves, or by increasing the spacing between the elements of the antenna arrays. An alternative approach to reducing the impact of high fading correlation on ITS-based MIMO systems is to apply relative delay offsets to the symbol streams transmitted from different antennas. This is discussed further in Section 4.4.

4.3 Slow fading

The simulation results discussed so far in this report were obtained with a channel model in which the channel matrix changes to a new, statistically independent realization after every symbol period, i.e., after every block of $N_t M_c$ code bits. Because channel coding and interleaving across

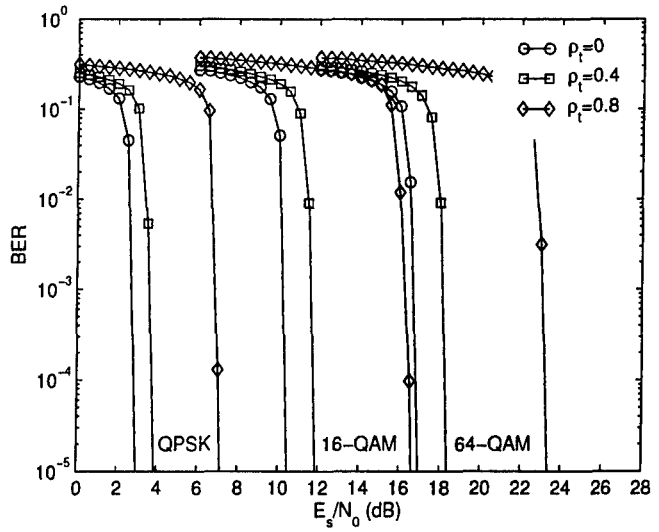

Figure 4.3. Error performance of a 4×4 ST-BICM MIMO system employing the MLM-ITS detector with $M = 8$, for different degrees of transmit fading correlation. Number of iterations in the detector/decoder loop is four. Channel code is a turbo code with rate 1/2 and memory 2.

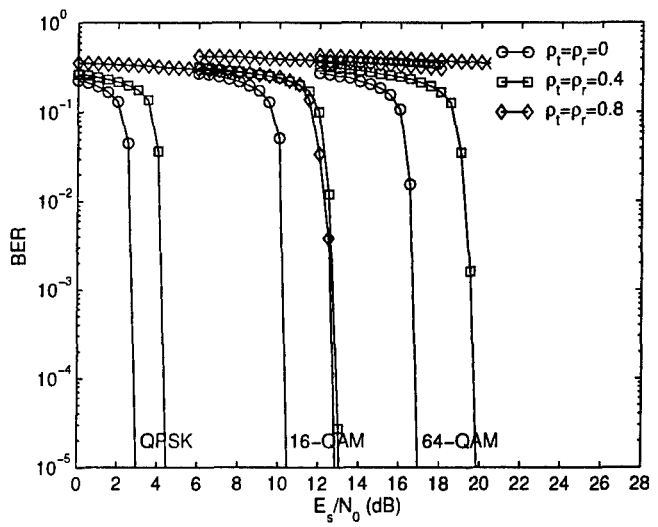

Figure 4.4. Error performance of a 4×4 ST-BICM MIMO system employing the MLM-ITS detector with $M = 8$, for different degrees of transmit and receive fading correlation. Number of iterations in the detector/decoder loop is four. Channel code is a turbo code with rate 1/2 and memory 2.

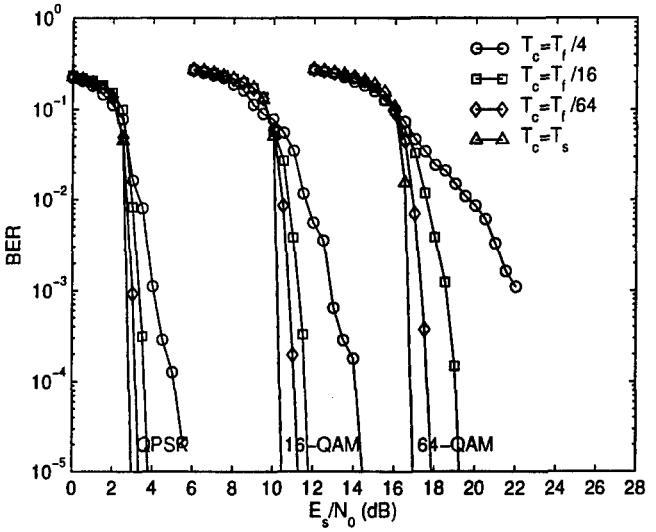

Figure 4.5. Error performance of a 4×4 ST-BICM MIMO system employing the MLM-ITS detector with $M = 8$, for different channel fading rates. Number of iterations in the detector/decoder loop is four. Channel code is a turbo code with rate 1/2 and memory 2.

rapid channel variations yields high temporal diversity, the performance results obtained with this model tend to be very good. Practical wireless systems are typically designed such that the channel coherence time T_c, which is the duration for which the channel remains unchanged for practical purposes, is large compared to the symbol period. This ensures that an accurate channel estimate can be obtained in the training interval, which remains reliable during the transmission of a large number of payload symbol vectors. If the coherence time is comparable to or larger than the frame duration, T_f, however, performance is degraded because no temporal diversity is available. In that case, channel realizations with few usable spatial eigenmodes [25, 26] are not compensated for by better channel realizations, and the probability of error is lower-limited by the probability that the instantaneous channel does not support the data throughput.

The dependency of the error performance of MLM-ITS detection on the number of constant-channel blocks per frame, i.e., on the ratio T_f/T_c, was investigated by means of simulations. Perfect channel estimation and uncorrelated fading were assumed. Fig. 4.5 shows results of these simulations for values of T_c equal to $T_f/64$, $T_f/16$ and $T_f/4$. The error performance corresponding to the rapid fading case of Section 3.5, for which $T_c = T_s$, is shown for reference. Considerable performance loss relative to $T_c = T_s$, ranging from approximately 3 dB for 4×4 QPSK to well over 5 dB for 4×4 64-QAM, is observed for $T_c = T_f/4$. For $T_c = T_f/16$, i.e., 16 constant-channel blocks per frame, performance degradation is limited to approximately 1 dB for 4×4 QPSK and approximately 2 dB for 4×4 64-QAM. Finally, for $T_c = T_f/64$, performance degradation is smaller than 1 dB for all cases considered here. It is also seen in Fig. 4.5 that the rate at which the bit error rate decreases with E_s/N_0 is smaller for configurations with lower diversity order, which is a well-known phenomenon [33]. In general, it can be concluded that sensitivity to a lack of temporal diversity increases as the signal constellation size becomes larger. In order to keep performance degradation small, i.e., smaller than 1 dB, the frame duration should be chosen between one and two orders of magnitude longer than the coherence time of the channel.

It is clear from the above discussion that, for a given frame duration and, hence, receiver delay, the performance of MIMO systems with perfect channel knowledge degrades if the channel coher-

ence time increases. In real-world MIMO systems, however, increasing coherence time enables more accurate channel estimation, which contributes to better error performance. If soft-decision feedback is used, this does not necessarily come at the cost of increased channel training overhead. It is therefore not possible to draw specific conclusions with regard to the effect of T_c on the performance of MIMO systems, and in particular the MLM-ITS detector, before a suitable channel estimation and tracking scheme has been developed. As discussed in Section 4.1, this is the subject of ongoing research. For a given coherence time, on the other hand, it is generally advisable to choose the frame duration T_f, and hence the interleaving delay, as long as can be tolerated within system requirements. The maximum interleaving delay that can be tolerated in practice depends on the application, but is typically in the range from 10 to 100 ms. In indoor environments, where the channel coherence time can be as high as 100 ms, considerable performance degradation should be anticipated unless alternative diversity techniques such as frequency diversity, discussed in Section 4.5, can be used.

4.4 Asynchronous reception

Literature on MIMO has hitherto dealt almost exclusively with synchronous reception, in which signals transmitted from different antennas are synchronized at the receiver. Generally, it is implicitly assumed that the antennas in the transmit and receive arrays are located sufficiently close to one another that the maximum difference in propagation delay between each transmit/receive antenna pair is very small compared to the symbol period. This means that the maximum coded bit rate must be smaller than approximately $N_t M_c c_0 / \Delta s$, where Δs is the maximum separation between any two transmit or receive antennas, and c_0 is the speed of light. For example, a 4×4 64-QAM MIMO system with maximum array dimensions of 1 m can be operated synchronously as long as the coded bit rate is much lower than approximately 7 Gbps, which is clearly not a limitation for current wireless communication systems. However, asynchronous scenarios can occur, for example, in the uplink of multiuser systems or in the downlink of networks with geographically distributed transmit arrays. In such scenarios, existing MIMO detection schemes, including (MLM-)ITS, can no longer be applied.

A scheme called asynchronous iterative trellis search (A-ITS) detection, which is suitable for asynchronous scenarios, was proposed and evaluated in [34]. Although the assumption of small separation between receive antennas was still made in [34], it is straightforward to modify the A-ITS detector in order to accommodate arbitrarily located transmit and receive antennas. The A-ITS detection scheme is similar to MLM-ITS detection in the sense that it employs the M-algorithm in order to search for the symbol sequences most likely to have been transmitted, given the received signal and any available *a priori* information. However, as its name indicates, this search is performed over a trellis instead of a tree structure. In the case of synchronous reception, the performance of the A-ITS detector is identical to that of the MLM-ITS detector. Interestingly, it has been shown that, in asynchronous scenarios, the performance of the A-ITS detector can be considerably better than in the synchronous case. This improvement can be explained by the fact that the correlation between symbols transmitted from different antennas is the result of both spatial and temporal correlation. Temporal correlation, which is determined by the "overlap" between the time intervals in which the different symbols are received, is at its maximum in the case of synchronous reception, and hence decreases when reception becomes asynchronous.

While spatial correlation is a consequence of the physical attributes of the channel and the antennas, temporal correlation can be controlled by adjusting the relative timing of the spatially multiplexed symbol streams at the transmitter. It can therefore be concluded that the performance

of MIMO systems can be improved considerably by purposely applying delay offsets to the parallel data streams. This has indeed been demonstrated in [34]. The moderately higher complexity associated with asynchronous detection is expected to be far outweighed by this performance improvement. This technique may be especially useful in the presence of highly correlated fading, where even small decreases in symbol correlation can lead to considerable performance improvement, as discussed in Section 4.2. Furthermore, this technique eliminates the requirement of (MLM-)ITS detection that $N_r \geq N_t$, which is necessary for the transformation of the channel matrix in triangular form, as discussed in Section 3. In A-ITS detection, it is guaranteed that the channel matrix relating the received signals to the transmitted symbols can be transformed to a band-limited lower triangular matrix as long as symbols are not fully correlated. This, in turn, is guaranteed if the data substreams transmitted from different antennas are not synchronized at the receiver.

4.5 Frequency-selective fading

So far it has been assumed that the MIMO channel is frequency non-selective over the system bandwidth, as reflected in the channel model (2.3). In real-world MIMO systems, however, the delay spread in the channel may be comparable to or larger than the symbol period T_s, which leads to inter-symbol interference. In practice, the delay spread typically ranges from approximately 100 ns in confined indoor environments to approximately 10 μs in hilly outdoor areas. This means that frequency-selective fading becomes significant at coded bit rates higher than approximately $N_t M_c$ times 0.1–10 MHz. depending on the application. For example, a 4 × 4 64-QAM indoor MIMO system would be considered wideband for coded bit rates higher than approximately 2 Mbps. The basic ITS and MLM-ITS detectors described in Section 3 are not directly applicable in wideband channels.

One approach to dealing with frequency-selective fading is to divide the system bandwidth up into smaller subbands, each of which smaller than the coherence bandwidth, which is usually defined as the inverse of the delay spread. The coded and interleaved bit stream is then serial-to-parallel converted into parallel streams, each of which is transmitted in a different subband. Transmission and reception in each subband proceeds in a manner identical as in the narrowband case of Section 3. This approach has been adopted in systems that are referred to as discrete matrix multitone (DMMT) and MIMO-OFDM [35–37]. Its main advantages are that it can be used in conjunction with narrowband MIMO detection schemes such as MLM-ITS detection, and has high robustness against frequency-selective fading and narrowband interference. Because the fading in the different subbands tends to be uncorrelated, this approach exploits the frequency diversity, sometimes also referred to as multipath diversity, inherent in wideband channels. Known practical problems with multi-carrier techniques include the need for extensive channel training and relatively long guard intervals, as well as the high peak-to-average power ratio of the combined signal, which reduces the efficiency of the power amplifier.

An alternative, single-carrier approach to dealing with frequency-selective fading is to have the detection scheme compensate for its effects in the time domain, using so-called adaptive equalization. A wideband MIMO channel is characterized in the time domain by multiple channel matrix taps, $\mathbf{H}(l)$, $l = 0, \cdots, L$, where the integer number L represents the maximum time delay spread, normalized to the symbol period T_s. The received signal is given by

$$\mathbf{y}(k) = \sum_{l=0}^{L} \mathbf{H}(l)\mathbf{s}(k-l) + \mathbf{n}(k), \tag{4.10}$$

where bracketed indices are now used to indicate the time-dependent nature of the variables $\mathbf{y}$, $\mathbf{H}$,

$\mathbf{s}$ and $\mathbf{n}$. Note that, apart from the time indices, (4.10) with $L = 0$ is identical to the narrowband channel model (2.3). For $L > 0$, the received signal vector depends not only on the symbol vector transmitted in the current symbol interval, but also on previously transmitted symbol vectors. As a consequence of this non-zero channel memory length, high-likelihood symbol vectors cannot be found by means of a tree search, as in narrowband MLM-ITS detection. Instead, a non-exhaustive trellis search can be employed, similar to that in asynchronous MIMO detection [34]. Although the maximum number of state transitions to be searched for each symbol would be no less than $2^{LN_tM_c}$, it is expected that a reduced-state trellis search would generally provide good results, especially since the matrix taps tend to be statistically independent, which results in a frequency diversity gain. A more detailed evaluation of trellis-search based adaptive equalization for MIMO, possibly in conjunction with asynchronous MIMO detection, is part of ongoing research.

5 Discussion and conclusions

This report has addressed the performance of iterative MIMO detection under real-world conditions including imperfect channel knowledge and spatially correlated and slow fading. Approaches to dealing with these non-ideal characteristics, as well as other real-world issues such as frequency-selective fading and non-synchronized reception were also addressed. The results of this study are relevant for the implementation of real-world ST-BICM MIMO wireless systems. Although the results presented herein are based on the (MLM-)ITS detection scheme, they are expected to be typical of most iterative MIMO detection schemes. The main conclusions of this report are related to channel estimation and the modification of the ITS scheme to enable wideband and asynchronous reception, as discussed next.

5.1 Channel estimation

The assumption of availability of perfect channel knowledge is the single least realistic one in the presentation of ITS detection in Section 3, and the development of a suitable MIMO channel estimation scheme is a necessity in the implementation of any practical MIMO system. Channel estimation by means of the transmission and processing of pilot symbol vectors and the use of soft decision feedback was discussed in Section 4.1. The simulation results in this section show that, if the coded bit rate is higher than approximately $100N_t^2M_c/T_c$, channel training alone is sufficient to obtain the same performance as with perfect channel knowledge. If the channel is rapidly changing, i.e., if the coded bit rate is lower than approximately $100N_t^2M_c/T_c$, a more sophisticated channel estimation scheme is required. As discussed in Section 4.1.2, feedback of the soft information generated by the detector is probably the most promising approach in that case. It is expected that it is possible to exploit a typical attribute of ITS detection, namely the fact that it generates a list of "good" symbol vectors and their log-likelihoods, to improve on existing soft-decision feedback schemes. Whereas existing schemes degrade system performance if reliable soft feedback is absent, the new scheme would weigh its channel estimation update based on the detection reliability of the current symbol vector. Channel estimation accuracy with soft decision feedback can thus not be worse than without.

The main drawback of the use of soft-decision feedback is its relatively high complexity, which is partly caused by the processing of a list of symbol vectors instead of a single, known pilot symbol vector, and also by the matrix inversion that is required to compute the channel estimate. It may be possible to reduce the complexity of the former task by limiting the number of candidate symbol vectors from which the channel is estimated. The matrix inversion can possibly be avoided by directly updating the channel estimate using a gradient descent approach, as in [24].

5.2 Enabling wideband and asynchronous reception

In certain high data rate applications, where multipath is severe or the separation between array elements is very large, propagation delay differences between multipath components or different pairs of transmit and receive antennas can become significant with respect to the symbol period. As discussed in Sections 4.4 and 4.5, the (MLM-)ITS detection scheme can not be applied in such situations. Instead, a trellis search based scheme referred to as A-ITS [34] could then be used. This

scheme is in many respects similar to MLM-ITS, but is capable of dealing with received symbols that overlap with both previously and subsequently received symbols.

In addition to mitigating the adverse effects of frequency-selective fading, it is expected that the A-ITS detection scheme can exploit the frequency diversity available in such channels, and therefore provide enhanced performance. This is particularly desirable in indoor applications, where, as discussed in Section 4.3, temporal diversity gain is typically low. It has been shown in [34] that considerable performance improvement relative to MLM-ITS can even be achieved in narrowband channels, by purposely applying delay offsets to the symbol streams transmitted from different antennas. This improvement is due to the lower symbol correlation resulting from the smaller temporal overlap between symbols, which is known to improve the efficiency of the breadth-first trellis search employed in both MLM-ITS and A-ITS detection. It is expected that asynchronous MIMO reception is especially beneficial in the case of severe spatial fading correlation, to which MLM-ITS is vulnerable, as discussed in Section 4.2. Furthermore, the use of A-ITS eliminates the limitation that the number of receive antennas should be at least equal to the number of transmit antennas, which makes the scheme more widely applicable, for example in transmit diversity systems.

A potential drawback of A-ITS detection is its moderately higher complexity. However, like MLM-ITS, A-ITS offers the possibility to trade off improved performance for lower complexity. It is expected that the complexity increase associated with asynchronous detection is far outweighed by the performance gain and other advantages mentioned above. Other issues that need to be addressed concerning A-ITS detection include the question whether, and how much, oversampling is required in order to deal with asynchronously received signals, as well as the problem of wideband and asynchronous channel estimation.

References

[1] Y.L.C. de Jong, "A reduced-complexity soft detector for iterative MIMO receivers," in *Proc. ANTEM 2002*, Montreal, QC, Canada, 2002, pp. 101–104.

[2] Y.L.C. de Jong and T.J. Willink, "Iterative tree search detection for MIMO wireless systems," in *Proc. VTC 2002-Fall*, Vancouver, BC, Canada, 2002, pp. 1041–1045.

[3] B.M. Hochwald and S. ten Brink, "Achieving near-capacity on a multiple-antenna channel," *IEEE Trans. Commun.*, vol. 51, no. 3, pp. 389–399, Mar. 2003.

[4] A.M. Tonello, "Array processing for simplified turbo decoding of interleaved space-time codes," in *Proc. VTC2001-Fall*, Atlantic City, NJ, 2001, vol. 3, pp. 1304–1308.

[5] A. Stefanov and T.M. Duman, "Turbo-coded modulation for systems with transmit and receive antenna diversity over block fading channels: system model, decoding approaches, and practical considerations," *IEEE J. Select. Areas Commun.*, vol. 19, no. 5, pp. 958–968, May 2001.

[6] M. Sellathurai and S. Haykin, "TURBO-BLAST for wireless communications: theory and experiments," *IEEE Trans. Signal Processing*, vol. 50, no. 10, pp. 2538–2546, Oct. 2002.

[7] T. Abe and T. Matsumoto, "Space-time turbo equalization in frequency selective MIMO channels," *IEEE Trans. Veh. Technol.*, vol. 52, no. 3, pp. 469–475, May 2003.

[8] Y.L.C. de Jong and T.J. Willink, "Iterative tree search detection for MIMO wireless systems," *submitted to IEEE Trans. Commun.*, 2003.

[9] L.R. Bahl, J. Cocke, F. Jelinek, and J. Raviv, "Optimal decoding of linear codes for minimizing symbol error rate," *IEEE Trans. Inform. Theory*, vol. IT-20, pp. 284–287, 1974.

[10] S. Benedetto, G. Montorsi, D. Divsalar, and F. Pollara, "Soft-input soft-output modules for the construction and distributed iterative decoding of code networks," *Eur. Trans. Telecommun.*, vol. 9, no. 2, pp. 155–172, 1998.

[11] S. ten Brink, "Convergence of iterative decoding," *Electr. Lett.*, vol. 35, no. 10, pp. 806–808, 1999.

[12] S. ten Brink, "Convergence behavior of iteratively decoded parallel concatenated codes," *IEEE Trans. Commun.*, vol. 49, no. 10, pp. 1727–1737, Oct. 2001.

[13] A. van Zelst, R. van Nee, and G.A. Awater, "Turbo-BLAST and its performance," in *Proc. VTC2001-Spring*, 2001, vol. 2, pp. 1282–1286.

[14] J.B. Anderson and S. Mohan, "Sequential coding algorithms: a survey and cost analysis," *IEEE Trans. Commun.*, vol. COM-32, no. 2, pp. 169–176, Feb. 1984.

[15] M.C. Reed, C.B. Schlegel, P.D. Alexander, and J.A. Asenstorfer, "Iterative multiuser detection for CDMA with FEC: near-single-user performance," *IEEE Trans. Commun.*, vol. 46, no. 12, pp. 1693–1699, Dec. 1998.

[16] L. Wei, L.K. Rasmussen, and R. Wyrwas, "Near optimum tree-search detection schemes for bit-synchronous multiuser CDMA systems over Gaussian and two-path Rayleigh-fading channels," *IEEE Trans. Commun.*, vol. 45, no. 6, pp. 691–700, June 1997.

[17] D.E. Knuth, *The art of computer programming, vol. III: sorting and searching*, Addison-Wesley, Reading, MA, 1973.

[18] P. Robertson, E. Villebrun, and P. Hoeher, "Comparison of optimal and sub-optimal MAP decoding algorithms operating in the log domain," in *Proc. ICC'95*, Seattle, WA, 1995, pp. 1009–1013.

[19] G.J. Foschini, "Layered space-time architecture for wireless communication in a fading environment when using multi-element antennas," *Bell Labs Tech. J.*, vol. 1, no. 2, pp. 41–59, 1996.

[20] G.D. Golden, C.J. Foschini, R.A. Valenzuela, and P.W. Wolniansky, "Detection algorithm and initial laboratory results using V-BLAST space-time communication architecture," *Electr. Lett.*, vol. 35, no. 1, pp. 14–16, 1999.

[21] B. Hassibi and B.M. Hochwald, "How much training is needed in multiple-antenna wireless links?," *IEEE Trans. Inform. Theory*, vol. 49, no. 4, pp. 951–963, Apr. 2003.

[22] M. Sandell, C. Luschi, P. Strauch, and R. Yan, "Iterative channel estimation using soft decision feedback," in *Proc. IEEE Global Telecommunications Conference (GLOBECOM 1998)*, Sydney, Australia, 1998, pp. 3728–3733.

[23] G.W.K. Colman, "A comparison of gradient and block adaptive array algorithm performance in different environments," in *Proc. IST-039/RSY-012 Joint SET/IST Symp.*, Chester, UK, 2003.

[24] S. Rajagopal, S. Bhashyam, J.R. Cavallaro, and B. Aazhang, "Real-time algorithms and architectures for multiuser channel estimation and detection in wireless base-station receivers," *IEEE Trans. Wireless Comm.*, vol. 1, no. 3, pp. 468–479, July 2002.

[25] E. Telatar, "Capacity of multiple-antenna Gaussian channels," *European Trans. Tel.*, vol. 10, no. 6, pp. 585–595, Nov./Dec. 1999.

[26] J. Bach Andersen, "Antenna arrays in mobile communications: gain, diversity, and channel capacity," *IEEE Antennas Propagat. Mag.*, vol. 42, no. 2, pp. 12–16, Apr. 2000.

[27] K.I. Pedersen, J.B. Andersen, J.P. Kermoal, and P. Mogensen, "A stochastic multiple-input-multiple-output radio channel model for evaluation of space-time coding algorithms," in *Proc. VTC2000-Fall*, Boston, MA, 2000, pp. 893–897.

[28] S.L. Loyka and J.R. Mosig, "Channel capacity of N-antenna BLAST architecture," *Electron. Lett.*, vol. 36, no. 7, pp. 660–661, 2000.

[29] D.-S. Shiu, G.J. Foschini, M.J. Gans, and J.M. Kahn, "Fading correlation and its effect on the capacity of multielement antenna systems," *IEEE Trans. Commun.*, vol. 48, no. 3, pp. 502–513, Mar. 2000.

[30] M.T. Ivrlac, W. Utschick, and J.A. Nossek, "Fading correlations in wireless MIMO communication systems," *IEEE J. Select. Areas Commun.*, vol. 21, no. 5, pp. 819–828, June 2003.

[31] D. Chizhik, G.J. Foschini, M.J. Gans, and R.A. Valenzuela, "Keyholes, correlations, and capacities of multielement transmit and receive antennas," *IEEE Trans. Wireless Comm.*, vol. 1, no. 2, pp. 361–368, Apr. 2002.

[32] D. Gesbert, H. Bölcskei, D.A. Gore, and A.J. Paulraj, "Outdoor MIMO wireless channels: models and performance prediction," *IEEE Trans. Commun.*, vol. 50, no. 12, 2002.

[33] J.G. Proakis, *Digital communications*, McGraw-Hill, New York, fourth edition, 2001.

[34] Y.L.C. de Jong and T.J. Willink, "Iterative trellis search detection for asynchronous MIMO systems," in *Proc. VTC 2003-Fall*, Orlando, FL, 2003.

[35] G.G. Raleigh and J.M. Cioffi, "Spatio-temporal coding for wireless communication," *IEEE Trans. Commun.*, , no. 3, pp. 357–366, Mar. 1998.

[36] R.S. Blum, Y. Li, J.H. Winters, and Q. Yan, "Improved space-time coding for MIMO-OFDM wireless communications," *IEEE Trans. Commun.*, vol. 49, no. 11, pp. 1873–1878, Nov. 2001.

[37] T.J. Willink, "MIMO OFDM for fixed wireless access," in *Proc. Wireless 2003*, Calgary, AB, Canada, 2003.

List of symbols

Throughout this report, the notation $\hat{s}$ is used to indicate an estimate of s. Upper and lower-case bold symbols denote matrices and vectors, respectively. Unless noted otherwise, the notations $s_{i,j}$ and s_i are used to denote the (i, j)th and the ith element of the generic matrix $\mathbf{S}$ and vector $\mathbf{s}$, respectively.

c_0	speed of light
E_s/N_0	SNR per receive antenna
$\mathbf{H}$	MIMO channel matrix
$\mathbf{H}(l)$	lth matrix tap of wideband MIMO channel
$I(\cdot;\cdot)$	mutual information
$\mathbb{J}_i$	set of indices j, $j \in \{1, \cdots, M_c\}$, for which $x_{i,j} = +1$
$\mathbb{J}_i^{(l)}$	set of indices j, $j \in \{2l-1, 2l\}$, for which $x_{i,j} = +1$
L	maximum propagation delay spread, normalized to T_s
$L(\cdot; I/O)$	channel decoder soft input/output
$\mathbf{L}$	lower triangular Cholesky factor of $\mathbf{H}^\dagger\mathbf{H}$
$\mathbb{L}$	candidate symbol vector list
$L_A(\cdot)$	prior information
$L_E(\cdot)$	extrinsic information
$L_{E,\text{clip}}$	extrinsic information clipping value
M	list size of M-algorithm
M_c	number of bits per symbol
N_p	number of pilot symbols
N_r	number of receive antennas
N_t	number of transmit antennas
$\mathbf{n}$	additive noise vector
$\mathcal{O}$	Landau's symbol

$p(\mathbf{s})$	likelihood of $\mathbf{s}$
$\mathbf{R}_r$	receive correlation matrix
$\mathbf{R}_s$	correlation matrix of $\mathbf{s}$
$\mathbf{R}_t$	transmit correlation matrix
$\mathbf{R}_y$	correlation matrix of $\mathbf{y}$
$\mathbf{R}_{ys}$	cross-correlation matrix of $\mathbf{y}$ and $\mathbf{s}$
$\mathbf{s}$	symbol vector, representing block of N_t symbols
$\tilde{\mathbf{s}}$	soft estimate of $\mathbf{s}$
$s^{(l)}$	"intermediate" signal point at level l
$\mathbf{s}_{p.i}$	ith pilot symbol vector
T_c	channel coherence time
T_f	frame duration
T_s	symbol period
$\mathbf{x}$	vector representing block of $N_t M_c$ bits
$\mathbf{x}_i$	vector representing ith $M_c \times 1$ subblock of $\mathbf{x}$
$x_{i.k}$	kth bit mapped onto ith symbol
$\mathbb{X}_{i.j}^{\pm 1}$	set of vectors $\mathbf{x}$ for which $x_{i.j} = \pm 1$
$\mathbf{y}$	received signal vector
$\mu(\mathbf{s})$	metric of $\mathbf{s}$, equal to log-likelihood of $\mathbf{s}$
μ_i	path metric at symbol depth i
$\mu_i^{(l)}$	path metric at level l of symbol depth i
Π	interleaving
ρ_r	receive correlation coefficient
ρ_t	transmit correlation coefficient
σ_n^2	noise variance
σ_s^2	average power per transmit antenna

List of abbreviations and acronyms

A-ITS	asynchronous ITS
APP	*a posteriori* probability
BCJR	Bahl-Cocke-Jelinek-Raviv (authors of BCJR algorithm)
BER	bit error rate
BLAST	Bell Labs layered space-time
CRC	Communications Research Centre Canada
DMMT	discrete matrix multitone
DND	Department of National Defence
DRDC	Defence R&D Canada
ITS	iterative tree/trellis search
LLR	log-likelihood ratio
MAP	maximum *a posteriori*
MIMO	multiple-input multiple-output
ML	maximum likelihood
MLM-ITS	multilevel mapping ITS
OFDM	orthogonal frequency division multiplexing
QAM	quadrature amplitude modulation
QPSK	quarternary phase-shift keying
SC-MMSE	soft-cancellation minimum mean squared error
SNR	signal-to-noise ratio
ST-BICM	space-time bit-interleaved coded modulation

DOCUMENT CONTROL DATA

(Security classification of title, body of abstract and indexing annotation must be entered when the overall document is classified)

1. ORIGINATOR (the name and address of the organization preparing the document. Organizations for whom the document was prepared, e.g. Establishment sponsoring a contractor's report, or tasking agency, are entered in section 8.)

Communications Research Centre Canada
3701 Carling Ave.
Ottawa, Ontario

2. SECURITY CLASSIFICATION (overall security classification of the document, including special warning terms if applicable)

UNCLASSIFIED

3. TITLE (the complete document title as indicated on the title page. Its classification should be indicated by the appropriate abbreviation (S,C or U) in parentheses after the title.)

On the implementation of iterative detection in real-world MIMO wireless systems (U)

4. AUTHORS (Last name, first name, middle initial)

de Jong, Yvo, L.C.

5. DATE OF PUBLICATION (month and year of publication of document)	6a. NO. OF PAGES (total containing information. Include Annexes, Appendices, etc.)	6b. NO. OF REFS (total cited in document)
December 2003	38	37

7. DESCRIPTIVE NOTES (the category of the document, e.g. technical report, technical note or memorandum. If appropriate, enter the type of report, e.g. interim, progress, summary, annual or final. Give the inclusive dates when a specific reporting period is covered.)

Technical Report

8. SPONSORING ACTIVITY (the name of the department project office or laboratory sponsoring the research and development. Include the address.)

Defence R&D Canada - Ottawa
3701 Carling Ave.
Ottawa, Ontario

9a. PROJECT OR GRANT NO. (if appropriate, the applicable research and development project or grant number under which the document was written. Please specify whether project or grant)	9b. CONTRACT NO. (if appropriate, the applicable number under which the document was written)
N/A	5CP

10a. ORIGINATOR'S DOCUMENT NUMBER (the official document number by which the document is identified by the originating activity. This number must be unique to this document.)	10b. OTHER DOCUMENT NOS. (Any other numbers which may be assigned this document either by the originator or by the sponsor)
CRC-RP-2003-009	DRDC OTTAWA TR 2003-242

11. DOCUMENT AVAILABILITY (any limitations on further dissemination of the document, other than those imposed by security classification)

(X) Unlimited distribution
( ) Distribution limited to defence departments and defence contractors; further distribution only as approved
( ) Distribution limited to defence departments and Canadian defence contractors; further distribution only as approved
( ) Distribution limited to government departments and agencies; further distribution only as approved
( ) Distribution limited to defence departments; further distribution only as approved
( ) Other (please specify):

12. DOCUMENT ANNOUNCEMENT (any limitation to the bibliographic announcement of this document. This will normally correspond to the Document Availability (11). However, where further distribution (beyond the audience specified in 11) is possible, a wider announcement audience may be selected.)

N/A

13. ABSTRACT (a brief and factual summary of the document. It may also appear elsewhere in the body of the document itself. It is highly desirable that the abstract of classified documents be unclassified. Each paragraph of the abstract shall begin with an indication of the security classification of the information in the paragraph (unless the document itself is unclassified) represented as (S), (C), or (U). It is not necessary to include here abstracts in both official languages unless the text is bilingual).

Theoretically, multiple-input multiple-output (MIMO) wireless systems can achieve remarkably high spectral efficiency as compared to conventional, single-antenna systems. This report identi-fies a number of problems which need to be solved in order to implement practical MIMO systems: channel estimation, correlated fading, slow fading, asynchronous reception, and frequency-selective fading. The effects of these non-ideal conditions on the performance of MIMO systems are eval-uated, and directions are explored in which solutions may be found. The focus of the report is on MIMO systems employing an iterative ("turbo") receiver. The results presented are based on the iterative tree search (ITS) detection scheme developed recently at CRC, but are expected to be typical of most iterative detectors that have been proposed in the MIMO literature. The main con-clusion of the report is that iterative channel estimation and further development of an ITS-based detection scheme for asynchronous and wideband reception are the two most promising topics for future research in this area.

14. KEYWORDS, DESCRIPTORS or IDENTIFIERS (technically meaningful terms or short phrases that characterize a document and could be helpful in cataloguing the document. They should be selected so that no security classification is required. Identifiers such as equipment model designation, trade name, military project code name, geographic location may also be included. If possible keywords should be selected from a published thesaurus. e.g. Thesaurus of Engineering and Scientific Terms (TEST) and that thesaurus-identified. If it is not possible to select indexing terms which are Unclassified, the classification of each should be indicated as with the title.)

MIMO systems, iterative detection/decoding, implementation issues